JUL 8 [redacted]
Grant No. 830-H-15 NAS 1.60:1871

NASA Technical Paper 1871

COMPLETED
ORIGINAL

Subsonic Tests of an All-Flush-Pressure-Orifice Air Data System

Terry J. Larson and Paul M. Siemers III

JUNE 1981

NASA

NASA Technical Paper 1871

Subsonic Tests of an All-Flush-Pressure-Orifice Air Data System

Terry J. Larson
Dryden Flight Research Center
Edwards, California

Paul M. Siemers III
Langley Research Center
Hampton, Virginia

National Aeronautics
and Space Administration

**Scientific and Technical
Information Branch**

1981

I

Blank Page

SUBSONIC TESTS OF AN ALL-FLUSH-PRESSURE-ORIFICE AIR DATA SYSTEM

Terry J. Larson
Dryden Flight Research Center

and

Paul M. Siemers III
Langley Research Center

INTRODUCTION

A flight and wind-tunnel test program is being conducted to investigate the feasibility of using all-flush-pressure-orifice air data systems (FADS) on aircraft at subsonic and transonic speeds (refs. 1 and 2). This program was initiated after investigations indicated that the shuttle entry air data system (SEADS), which was originally planned for limited air data measurements at supersonic and hypersonic speeds (ref. 3) might also be useful at lower speeds, as well as for aircraft other than the shuttle orbiter (refs. 4 to 6). Air data systems that consist only of flush orifices installed directly on the skin of the vehicle can minimize the structural and other installation problems associated with nose-boom probes.

To investigate the subsonic performance of FADS, both a full-scale airplane and a 0.035-scale model of the KC-135A airplane were provided with orifices. Tests were conducted with the airplane in flight at the NASA Dryden Flight Research Center and with the model in the 8-Foot Transonic Pressure Tunnel at the NASA Langley Research Center (ref. 1). Various combinations of pressure orifices were investigated, but all were in one of two basic configurations: on the nose of the vehicle only and on both the nose and the sides of the fuselage. The 18 orifices on the nose of the vehicle and model were in a cruciform pattern similar to that of the SEADS nose orifices. The wind-tunnel tests were conducted at Mach numbers from 0.3 to 0.9, angles of attack from -2° to 16°, and angles of sideslip of 0° and 5°. The full-scale KC-135A airplane flight data were obtained during two test flights for narrower ranges of Mach number and angle of attack and for a larger range of angle of sideslip. As reported in refer-

ence 2, the flight and wind-tunnel tests showed that the system can provide the same air data quantities as a conventional pitot-static and flow angularity system.

In addition to data first presented in reference 2, this paper compares the air data quantities derived from FADS pressure measurements on the second test flight with air data derived from the airplane's calibrated conventional pitot-static and flow angularity sensors. The FADS quantities were derived by using two procedures, one of which used pressure relationships developed from the first test flight and the second of which used pressure relationships developed from the wind-tunnel data (ref. 1). The FADS quantities were derived from selected orifices, rather than from all of those available, unlike the procedure proposed for the derivation of air data from SEADS at supersonic and hypersonic speeds in references 7 and 8.

SYMBOLS AND ABBREVIATIONS

a_x	longitudinal acceleration, g
CRT	cathode ray tube
FADS	flush air data system
h_p	pressure altitude, geopotential km
M	Mach number
M_{ic}	indicated Mach number corrected for instrument error
PCM	pulse code modulation
p_i	pressure measured at ith orifice (i = 1 to 22 (fig. 3)), kPa
p_{lower}	pressure measured on lower surface of nose, kPa
p_{meas}	pressure measured on surface of nose between orifices that measure p_{lower} and p_{upper}, kPa
p_t	total pressure, kPa
p_{upper}	pressure measured on upper surface of nose, kPa
$p_{21,22}$	pressure measured from static pressure orifices 21 and 22 of airplane and model; pressures were measured from manifolded orifices on the airplane and were averaged from the two orifices on the model, kPa
q	dynamic pressure, kPa

SEADS	shuttle entry air data system
x, y, z	longitudinal, lateral, and vertical coordinates, respectively (fig. 3), cm
α	corrected angle of attack, deg
α_v	angle of attack indicated by reference vane, deg
β	corrected angle of sideslip, deg
β_v	angle of sideslip indicated by reference vane, deg
Δp_α	pressure differential between two orifices in angle of attack plane, kPa
Δp_β	pressure differential between two orifices in angle of sideslip plane, kPa
τ_α	angle of attack parameter, $\dfrac{p_{lower} - p_{upper}}{(p_{meas} - p_{lower}) + 0.5(p_{lower} - p_{upper})}$

TEST CONFIGURATION AND CONDITIONS

Test Configuration

Tests were performed on a full-scale KC-135A airplane and a full-span 0.035-scale model of the airplane. The flight tests were performed at the NASA Dryden Flight Research Center with a KC-135A airplane operated by the NASA Johnson Space Center. A photograph of the airplane is shown in figure 1, and its physical dimensions are shown in figure 2. The wind-tunnel tests (ref. 1) were conducted in the 8-Foot Transonic Pressure Tunnel at the NASA Langley Research Center, which is described in reference 9.

The nose of both the airplane and the model are equipped with 18 pressure measurement orifices installed in identical locations. The orifices are arranged in a cruciform pattern located along the vertical and longitudinal body axes (fig. 3). The airplane orifices are 0.32 centimeter in diameter, and the model orifices are 0.076 centimeter in diameter. Except for the three upper orifices, the arrangement of the orifices in the vertical plane of symmetry (fig. 3(a)) closely approximates a circular arc. The arrangement of all seven orifices in the horizontal plane of symmetry (fig. 3(b)) also approximates a circular arc. The cruciform pattern of the nose orifice array is similar to that of the SEADS nose cap orifices. The SEADS orifices in the horizontal plane, however, are displaced from the horizontal centerline because of structural considerations.

On the airplane and model, there were two orifices on the sides of the fuselage that were designated orifices 21 and 22 (fig. 3(c)) in addition to the nose orifices. On

the airplane, these orifices were manifolded to provide a measurement of static pressure and the orifices corresponded to the airplane's standard static pressure source. Orifices 21 and 22 on the model were not manifolded.

The wind-tunnel model (fig. 4), unlike the test airplane, was equipped with winglets that were installed for an unrelated investigation. The winglets are not believed to affect the results presented in this paper.

Test Conditions

As shown in table 1, maneuvers were flown at various Mach numbers and altitudes to evaluate FADS during the flight program. The tests at constant Mach numbers and pressure altitudes and the level accelerations and decelerations were flown for two purposes: to evaluate the calibration of the reference static pressure system (orifices 21 and 22) and to evaluate the effect of Mach number on FADS. The other maneuvers were flown to evaluate the effects of changes in angle of attack and angle of sideslip on FADS. The test data from these maneuvers that were used in the subsequent flight/wind-tunnel comparisons generally were selected to match the wind-tunnel conditions as closely as possible. Except for the data from the level accelerations and decelerations, data were also selected for quasi-steady flight conditions to minimize pneumatic lag effects. Special care was taken to select data for which angle of attack and angle of sideslip were constant because of the changes in pressure that are associated with flow angle variation.

The wind-tunnel tests were conducted at five Mach numbers (0.3, 0.5, 0.7, 0.78, and 0.9). Angle of attack was varied in 2° increments from -2° to 16°. Data were obtained for angles of sideslip of both 0° and 5°. Because of excessive model vibration, which increased with both Mach number and angle of attack, data were not obtained at angles of attack above 10° and 8° for Mach numbers of 0.78 and 0.90, respectively.

Reynolds number varied between 4.43×10^6 per meter and 10.95×10^6 per meter for the flight tests and between 2.6×10^6 per meter and 9.1×10^6 per meter for the wind-tunnel tests.

MEASUREMENT DESCRIPTION AND ACCURACY

To provide a reference static pressure for the full-scale airplane, the copilot's static pressure orifices (fig. 3(c)) were used. These orifices were pneumatically manifolded. These fuselage orifices also served as orifices 21 and 22 in the FADS for the airplane. The reference static pressures were corrected for position error from flight calibration data as described in the appendix. The reference total pressure was measured from the copilot's pitot probe on the left side of the fuselage. On the basis of calibration data for an identical installation on a different KC-135A airplane flown at Dryden, total pressure position error corrections were considered unnecessary.

A wedge-shaped pivoting angle of attack vane was installed on the right side of the fuselage, and a similar angle of sideslip vane was mounted 10 centimeters left of the bottom centerline of the fuselage. These vanes were used for reference flow angle measurements. A sensitive longitudinal accelerometer at the center of gravity of the airplane was used for calibrating the angle of attack measurements. A more detailed description of the vane calibration procedure is given in the appendix.

Force-balance digital pressure transducers were used to provide reference measurements of pressure altitude and airspeed (fig. 5). The pressure altitude transducer was also used to provide the reference pressure for the FADS differential pressure measurements. Each of the 18 FADS pressure orifices on the nose was connected to a differential pressure transducer by less than 3.1 meters of 0.32-centimeter-inside-diameter tubing (fig. 6). The pulse code modulation (PCM) data instrumentation package was mounted on a pallet installed in the airplane (fig. 7). Data were recorded on board the airplane on magnetic tape and also telemetered to the ground, where real-time monitoring was conducted by utilizing cathode ray tube (CRT) display and strip chart recording. A time-code generator and a C-band radar transponder for FPS-16 radar tracking completed the instrumentation. The FADS flight test measurements, the associated ranges, and estimates of 2σ accuracy are listed in table 2.

Estimates of accuracy were derived for both the reference measurements and the FADS pressure ratios by considering all the error sources. Uncertainties of 2σ (table 2) were estimated for the reference quantities by including instrument errors, recording errors, and uncertainties in the position error calibrations. The resulting uncertainties in Mach number and angle of attack are ± 0.005 and $\pm 0.5°$, respectively. Because of the significant sidewash on the sideslip vane and its variation with angle of attack, the 2σ uncertainty in angle of sideslip is $\pm 0.75°$. Uncertainties of 2σ in the most important FADS pressure ratios were derived by using a root-sum-square analysis and are shown for selected test conditions in table 3.

RESULTS AND DISCUSSION

The FADS pressure relationships for the determination of total pressure, angle of attack, angle of sideslip, and Mach number are presented in figures 8 to 17. Iteration solutions are required for derivation of the air data quantities from these relationships. Results are presented only for 0° of angle of sideslip except for the evaluation of the pressure parameter used for the determination of sideslip.

Total Pressure

The ratio of the FADS-measured pressures to the reference total pressure, p_i/p_t, is plotted against Mach number for three angles of attack in figure 8. The FADS measurements were made at nine orifices in the vertical plane of symmetry (orifices 4 to 12). Data for orifices 4 to 7 are shown in the upper plots; data for orifices 8 to 12 are in the lower plots. The wind-tunnel data are faired, except for

the wind-tunnel data for orifices 4 to 6 in figure 8(a), which are not faired to prevent overcrowding. For all of these orifices, the difference between the flight and wind-tunnel data is well within 0.01. Some difference can be expected, of course, because of measurement error (table 3). However, the maximum difference for any FADS nose pressure orifice is equivalent to a displacement from the intended orifice location on the small-scale model of less than one orifice diameter (0.076 cm), which is about the placement tolerance for the orifices.

A comparison of figures 8(a), 8(b), and 8(c) shows that the pressure ratios are significantly affected by variations in both Mach number and angle of attack. Orifice 12 shows the largest variation with both Mach number and angle of attack and is therefore the least suitable orifice for the determination of total pressure. However, several orifices show little variation with angle of attack and Mach number. In figure 9, values of a total pressure term $\Delta p_t/p_t$ based on the wind-tunnel data are plotted against Mach number for several angles of attack for three of these orifices (orifices 6, 7, and 8). Orifice 8 provides the pressure values that require the least amount of correction for the range of test conditions shown. However, when angle of attack is limited to the usual operating range of the KC-135A airplane (-2° to 8°), orifices 6 and 7 require smaller corrections and would therefore be preferable to orifice 8.

Angle of Attack and Angle of Sideslip

Angle of attack and angle of sideslip can be correlated with pressure measurements from orifices in the vertical and horizontal planes, respectively. The parameters used to translate the pressure measurements to flow angle must have adequate sensitivity to flow angle and, ideally, should also be linear with changes in flow angle. Furthermore, the parameter should be little affected by other variables, such as Mach number. Two pressure parameters were investigated in reference 1 for the determination of angle of attack from FADS measurements. The first of these was the parameter $\Delta p_\alpha/q$, which is the difference in pressure between two orifices in the vertical plane of symmetry normalized by dynamic pressure. The second (refs. 10 and 11) was referred to as the τ parameter and is made up of three pressure measurements. This report evaluates both of these parameters further.

Figures 10(a) and 10(b) show the $\Delta p_\alpha/q$ parameter for selected orifice pairs plotted against angle of attack as calculated from flight data at Mach numbers of 0.5 and 0.7, respectively. Dynamic pressure, q, is calculated from the reference measurements of total pressure and static pressure. The upper plots in the figures show pairings with orifice 3, and the lower plots show pairings with orifice 6. Many other common orifices could have been selected, but, as will become clear in the following discussion, the matrix provided by these two includes several pairs that allow the accurate determination of angle of attack with the $\Delta p_\alpha/q$ parameter. Straight lines have been drawn through the data in figures 10(a) and 10(b) for all orifice pairs except (3, 7) and (3, 8). The small scatter from the straight line fairings indicates that the pressure parameter is nearly linear for most of the pairs. The curve slopes, which are shown in the legends, were calculated by using the end points of the curves. Pairs that include orifice 3 provide the largest sensitivity (slope) because the sensi-

tivity of $\Delta p_\alpha/q$ to angle of attack increases with measurement spacing. The minimum necessary sensitivity, of course, is dictated by required angle of attack accuracy, pressure transducer accuracy, and minimum expected dynamic pressure.

Figure 11 compares the flight values of $\Delta p_\alpha/q$ presented in figure 10(a) with the wind-tunnel values. The differences are notable for some of the orifice pairs. Again, however, these differences are within the orifice location tolerances noted in regard to the total pressure ratio values (fig. 8).

The wind-tunnel data reported in reference 1 and shown in figure 11(b) suggest that orifice pairs (6, 11) and (6, 12) perform best for angle of attack measurement if both the linearity and the sensitivity of the relationship between $\Delta p_\alpha/q$ and angle of attack are considered. The flight data, however, show that orifice pairs (3, 11) and (3, 12) (fig. 11(a)) provide not only the best sensitivity of the orifice pairs investigated, but also better linearity than indicated by the wind-tunnel data.

The wind-tunnel data in reference 1 show that the sensitivity (slope) of the pressure parameter $\Delta p_\alpha/q$ to angle of attack decreases with Mach number. The variation of the sensitivity with Mach number for orifice pairs (6, 11) and (6, 12) is presented in figure 12. The slopes are calculated by using the end points of the curves of $\Delta p_\alpha/q$ plotted against angle of attack. The flight-derived slopes agree fairly well with the wind-tunnel slopes for orifice pair (6, 11), but they are displaced by more than 0.01 for orifice pair (6, 12). Both sets of data, however, show dependence on Mach number, which is characteristic of this parameter when it is used with sensors used for measuring flow angles (ref. 12).

The other pressure parameter investigated in reference 1 for determining flow angularity, designated τ, has the advantage of being relatively insensitive to Mach number. Figure 13 shows this parameter for angle of attack determination, designated τ_α, plotted against angle of attack for two combinations of orifices. In comparing the two pressure parameters, the data show that the τ_α parameter is indeed less sensitive to Mach number but that it is also less linear with changes in angle of attack.

The authors conclude that either $\Delta p_\alpha/q$ or τ_α could be used for the accurate determination of angle of attack for the KC-135A airplane. In fact, the data indicate that many pairs of orifices could be used for angle of attack determination, which offers opportunities for redundant measurements and the statistical averaging of the measurements and lessens the impact of possible structural limitations on orifice location.

Angle of sideslip can be determined similarly from orifice pairs located in the horizontal plane. Figure 14 shows flight-determined values of $\Delta p_\beta/q$ plotted against angle of sideslip at several Mach numbers for orifice pairs (15, 16) and (14, 17). Only flight data are shown in the plots, because the wind-tunnel data were limited to 0° and 5° of sideslip. Data from orifices 13 and 18 are not shown because the installation of one of these orifices was found to be faulty. The sideslip pressure

parameter shows good linearity and sensitivity and very little variation with Mach number. Shown in the legends are the slopes of the pressure parameter when plotted against sideslip. Wind-tunnel values are also shown where the data are available (figs. 14(c) and 14(d)). The slopes of pressure parameters derived from the flight and wind-tunnel data agree within 10 percent, even though the wind-tunnel data were limited to two angles of sideslip. Orifice pair (14, 17) provides better sensitivity because of the larger separation of the orifices.

Mach Number

Pressure ratios for the determination of Mach number were derived from both flight and wind-tunnel data. Pressure ratios were derived from orifice pairs located on both the nose and on the fuselage as well as from pairs restricted to the nose. The pressure ratio $p_7/p_{21,22}$, which uses orifices both on the nose (7) and on the fuselage (21 and 22), is shown plotted against Mach number for various angles of attack in figure 15. The maximum difference in Mach number between the flight and wind-tunnel values for a given pressure ratio is less than 0.03. It is obvious from the figure that the sensitivity of this ratio to Mach number is adequate, as could be expected, since these pressures (p_7 and $p_{21,22}$) are close approximations of total and static pressure, respectively. The variation of the pressure ratio with angle of attack is quite small for angles below 8°. This results not only because of the small sensitivity of the pressures to angle of attack but also because the pressure ratio $p_7/p_{21,22}$ is less affected by change in angle of attack than the individual pressures (p_7 and $p_{21,22}$). The small sensitivity of the pressure ratio to angles of attack below 8° is advantageous for application to the KC-135A airplane, which normally flies at angles of attack less than 8°.

For the determination of Mach number from pressures measured exclusively on the nose, the data indicate that the most satisfactory pressure ratio is p_6/p_1. The all-nose-orifice configuration is of interest for flight vehicles for which orifice installations at locations aft of the nose are constrained. As shown in figure 16, the maximum difference in Mach number between the flight data and the wind-tunnel data is approximately 0.035, which is only slightly greater than the difference using $p_7/p_{21,22}$ (fig. 15). The data show, however, that a much larger angle of attack dependence results when two pressures from the nose are used for Mach number determination. The p_6/p_1 ratio can still provide reasonable Mach number information, since data scatter is not excessive and pressure ratio sensitivity is adequate. Moreover, the small variation of the pressure ratio with angle of attack at angles above 10° is of interest for application to vehicles that fly at high angles of attack, such as the space shuttle orbiter.

FADS Verification

To verify data acquired with FADS, air data derived from FADS data taken during the second test flight were compared with quantities from the reference air data system.

Two FADS values were obtained for each time, one by using calibration curves generated from the first flight test, and another by using calibration curves generated from the wind-tunnel tests (ref. 1). Some differences between the two calibrations can be expected, of course, because of instrumentation errors, nonrepeatable effects, and calibration errors in both systems.

Figure 17 shows time histories of Mach number, pressure altitude, and angle of attack as determined from the reference system for the quasi-level acceleration and the pushover pullup maneuver that were used in this comparison. FADS data were calculated every 2 seconds for the level acceleration and every single second for the pushover pullup maneuver. The differences between the reference and FADS values are presented in figures 18 and 19. Part (a) in both figures is for FADS air data quantities derived from orifices on both the nose and fuselage. Part (b) in the figures shows FADS air data quantities derived from nose orifices only. Orifices 6 and 12 were used for the determination of angle of attack in each case. In two instances (figs. 18(a) and 19(a)), orifices 3 and 12 were used as well. For convenience, table 4 presents the ranges of difference between FADS and reference system air data quantities based on both the flight and the wind-tunnel calibrations for the two maneuvers.

Because of the number of comparisons to be made, the following discussion will first be limited to comparisons for which FADS quantities were derived by using calibrations based on the first flight (solid lines in figs. 18 and 19). In the data for the level acceleration maneuver (fig. 18), it is apparent that the maximum absolute differences in Mach number, pressure altitude, and angle of attack (using p_6 and p_{12}) are 0.01, 60 meters, and 0.5°, respectively, regardless which FADS configuration is used. The maximum difference in angle of attack is only 0.2° when p_3 and p_{12} are used for Δp_α. Improvement over the accuracy obtained from orifices 3 and 12 is expected from the flight tests, as discussed previously. Systematic errors in addition to random errors are evident in the Mach numbers and pressure altitudes determined from FADS measurements. For example, the average Mach number difference at Mach numbers less than 0.5 (before a time of 40 seconds) is greater than 0.005, but it is close to 0 at the higher Mach numbers. Because of the significant dependence of the calculation of pressure altitude on Mach number, the differences in pressure altitude behave similarly to those for Mach number.

For the all-nose-orifice FADS configuration, the Mach number and pressure altitude differences (fig. 18(b)) are generally larger than those for the FADS configuration using both nose and fuselage orifices (fig. 18(a)). Angle of attack performance, however, is about equal.

The results of the pushover pullup maneuver (fig. 19), which was made at a Mach number of about 0.5, show that the Mach number differences based on the flight calibration vary considerably more for the all-nose-orifice configuration (fig. 19(b)) than for the configuration with both nose and fuselage orifices. This is to be expected when angle of attack varies, even if Mach number is constant, because of the dependence of the Mach number derivation on angle of attack, especially at lower angles (fig. 16). The Mach number differences for the FADS configuration with both nose and fuselage orifices (fig. 19(a)) are small and show little variation.

The ability of both FADS configurations to measure angle of attack is quite good for this maneuver, especially in view of the large changes in angle of attack and altitude (and thus Δp_q and q) during the maneuver.

The two test mancuvers indicate that air data derived from the optimum nose and fuselage orifice configuration generally compare more favorably with the data obtained from the reference air data system than do those of the optimum all-nose-orifice configuration. However, the performance of the two FADS configurations were quite similar in those maneuvers as measured by their maximum absolute data differences from the reference air data system. These differences for the optimum nose and fuselage orifice configuration were 0.01, 55 meters, and 0.6° for Mach number, pressure altitude, and angle of attack, respectively. These values compare quite closely with the corresponding differences for the all-nose-orifice configuration, which were 0.01, 60 meters, and 0.7°, respectively.

The differences between the FADS air data quantities and the calibration curves generated from the wind-tunnel data (dashed curves in figs. 18 and 19) are generally larger than the differences between the FADS air data quantities and the flight calibration curves. The maximum absolute differences between the optimum nose and fuselage orifice configuration air data measurements and the reference air data measurements were 0.025, 165 meters, and 1.0°, for Mach number, pressure altitude, and angle of attack, respectively. The corresponding differences for the all-nose-orifice configuration were 0.026, 170 meters, and 0.8°, respectively. Somewhat unexpectedly, for the pushover pullup maneuver (fig. 19), the configuration that uses nose orifices only agrees better with the reference measurements than the configuration that uses both nose and fuselage orifices. It can be assumed that the wind-tunnel calibration for the all-nose-orifice configuration is more accurate at this Mach number (0.5) than that for the other configuration.

The results of the comparison indicate how accurately a FADS can be expected to perform for aircraft similar to the KC-135A configuration. The results also indicate the degree of confidence that can be expected for calibrations based on wind-tunnel data, which will be the only data available for the initial flight use of SEADS. The orifices that are recommended on the basis of both the flight and wind-tunnel studies for the KC-135A configuration are summarized in table 5. However, as previously stated, additional or other orifices could also be used if they were needed to satisfy other requirements, such as a requirement for redundant measurements.

The limited flight and wind-tunnel tests reported here are sufficient to indicate that flush orifice air data systems are feasible. By implementing a more exhaustive calibration, it would be possible to minimize calibration uncertainties to the extent that FADS accuracy would be essentially limited by the accuracy of the pressure sensors used. The next section discusses the sensitivity of FADS to instrument error; that is, the accuracy that could be achieved if all calibration error could be removed.

Potential FADS Accuracy

In this study, the potential accuracy of FADS-derived quantities of Mach number, pressure altitude, and angle of attack was investigated by using calibration relation-

ships obtained from the wind-tunnel tests and a root sum square analysis. Angle of attack was determined by using the $\Delta p_\alpha/q$ parameter. As before, one configuration investigated used nose orifices only, whereas the other combined nose and fuselage orifices. The orifices selected are those recommended on the basis of the wind-tunnel measurements (table 5).

For this analysis, it was assumed that the only source of error was instrument error (which was assigned a value of ±0.05 kPa for all pressure measurements). Calibration errors were disregarded, and the results of the analysis were interpreted as the best accuracy that could be obtained with the FADS for the KC-135A configuration.

To provide a basis for comparison, a similar error analysis was also performed for what will be referred to as an "optimum" system—a system that uses a conventional pitot-static air data probe. As for FADS, an instrument error of ±0.05 kPa was assumed. Static and total pressure position errors for the pitot-static system were assumed to be 0. Because of the difficulty of defining a conventional flow angle measurement system and the variation of the flow angle errors with flight conditions, no attempt was made to derive angle of attack errors for a conventional system.

The analysis was performed over the KC-135A Mach number/altitude flight envelope for angles of attack of -2°, 8°, and 16°. Angle of sideslip was assumed to be 0°. Some results of the error analysis are shown in figures 20 and 22. Isolines of the errors (or uncertainties) are presented within the flight envelope. The Mach number and pressure altitude uncertainties for the "optimum" system are shown in figure 20. As expected, the Mach number uncertainties vary with Mach number and pressure altitude.

Figure 21 shows the uncertainties for a FADS that uses orifices on both the nose and the fuselage. The Mach number uncertainties are almost identical to those of the "optimum" system. The pressure altitude errors are slightly larger than those of the "optimum" system because of the dependence of these errors on Mach number. Angle of attack uncertainties increase as Mach number decreases at a given altitude because of the dependence of the angle of attack derivation on dynamic pressure. In general, the FADS uncertainties are small and are comparable to those for conventional angle of attack sensors.

Air data uncertainties for a FADS that uses orifices on the nose only are shown in figure 22. The results are shown for all three angles of attack because the uncertainties varied significantly with angle of attack. At an angle of attack of -2° (fig. 22(a)), the Mach number errors are approximately twice those of the "optimum" system. Agreement is much closer at the higher angles of attack, however. The pressure altitude uncertainties are significantly more than those of the "optimum" system at angles of attack of -2° and 8°; however, the FADS performs much better at an angle of attack of 16°. Figure 22(c) shows that the angle of attack uncertainties are nearly constant with changes in angle of attack and are about the same as those for the FADS with both nose and fuselage orifices (fig. 21(c)).

CONCLUDING REMARKS

An all-flush-pressure-orifice air data system (FADS) was evaluated at subsonic speeds using a KC-135A airplane in flight and a 0.035-scale model in wind-tunnel tests. Two orifice configurations were investigated, one with orifices on both the nose and the fuselage and the other with orifices on the nose only. The all-nose-orifice configuration was similar to the orifice configuration used in the shuttle entry air data system (SEADS), which was designed for supersonic and hypersonic flight conditions.

It was found that all of the air data quantities derived from conventional pitot-static and flow angularity measuring systems (total pressure, angle of attack, angle of sideslip, and Mach number) could be determined with a FADS. Several orifices on the vertical centerline of the nose of the vehicle were satisfactory for the determination of total pressure; the optimum orifice location depended on the aircraft's usual operating angle of attack range. Several orifice pairs on the vertical centerline provided pressure differentials that were satisfactory for the determination of angle of attack. Similarly, angle of sideslip could be determined from differential pressure measurements from orifice pairs on the aircraft's horizontal centerline. The best orifice configuration for the determination of Mach number utilized two manifolded orifices (one on each side of the fuselage) and one orifice on the nose. Orifice pairs confined to the nose could also be used for Mach number determination, but they were more sensitive to angle of attack, especially at low angles.

The FADS air data quantities derived using the optimum nose and fuselage orifice configuration were compared with those from a reference calibrated pitot-static and angle of attack measuring system. When calibration curves based on flight data were used, the largest absolute differences in Mach number, pressure altitude, and angle of attack were 0.01, 55 meters, and 0.6°, respectively. When wind-tunnel calibration curves were used, the corresponding differences were 0.025, 165 meters, and 1.0°, respectively. When the all-nose-orifice FADS configuration was used with the flight curves, the largest absolute differences in Mach number, pressure altitude, and angle of attack were 0.01, 60 meters, and 0.7°, respectively. When the wind-tunnel calibration curves were used, the corresponding differences were 0.026, 170 meters, and 0.8°, respectively.

The results demonstrated that a FADS can be successfully calibrated at subsonic speeds. They also indicate the accuracy that may be expected for air data derived with SEADS during space shuttle flight and pressure relationships developed from the wind-tunnel tests.

An analytical error analysis reveals that if calibration errors were eliminated and only instrument errors remained, a FADS made up of both nose and fuselage orifices approaches the performance of an "optimum" pitot-static system. Accuracy decreases when the FADS is limited to the nose orifices because of increased sensitivity to flow angle.

Dryden Flight Research Center
National Aeronautics and Space Administration
Edwards, California, December 29, 1980

APPENDIX—CALIBRATION OF REFERENCE AIR DATA SYSTEM

The static pressure position error calibrations for the FADS flight tests are shown in figure 23. The primary calibration techniques used are the Pacer method (ref. 13) and the radar tracking method (ref. 14). The latter is used with level accelerations and decelerations. A third method used airplane altitude determined by FPS-16 radar and rawinsonde pressure altitude data (ref. 14). No discernible angle of attack dependence was evident for the angles flown during the calibration tests. The fairing shown in figure 23 is taken from reference 15. Since it agrees quite closely with the flight data, it was used for data reduction.

The angle of attack vane and angle of sideslip vane measurements were corrected by using data from the airplane used in the FADS tests and from identical vanes installed on a second KC-135A airplane that was flown in an unrelated investigation. The resulting calibration for angle of attack, which is shown in figure 24, was obtained by equating the arc sine of the longitudinal acceleration at the airplane center of gravity during zero acceleration/constant altitude flight to the angle of attack (that is, α = Pitch angle = $\sin^{-1}\alpha_x$). No Mach number dependence was found.

The calibration for the reference angle of sideslip vane on the airplane used in the FADS tests was based on measurements from the angle of sideslip vane mounted on the nose boom of the second KC-135A airplane used in the separate investigation. Because the FADS airplane vane was mounted about 10 centimeters left of the lower fuselage centerline, significant sidewash was present in the calibration, as shown in figure 25. The correction to angle of sideslip also varied with the measured angle of attack. This was further investigated in the FADS flight tests, with the results shown in figure 26. The indicated angles of sideslip are plotted against the indicated angles of attack for several level acceleration and deceleration runs. For these runs it was assumed that the true angle of sideslip was constant at 0°. The differences in the magnitudes of the corrections indicate that the true angle of sideslip may have varied by as much as ±0.25° between runs. The slope of figure 25 for sidewash effect, and an average slope and intercept from figure 26 for the angle of attack effect, were used to obtain the following equation.

$$\beta = 0.577(\beta_v - 0.204\alpha_v - 6.0)$$

This equation was used to correct the vane measurements to obtain reference sideslip values in degrees for the FADS investigation.

REFERENCES

1. Larson, Terry J.; Flechner, Stuart G.; and Siemers, Paul M. III: Wind Tunnel Investigation of an All Flush Orifice Air Data System for a Large Subsonic Aircraft. NASA TP-1642, 1980.

2. Larson, Terry J.; and Siemers, Paul M. III: Subsonic Investigation of an All Flush Orifice Air Data System. Proc. 1980 Air Data Systems Conf. (Colorado Springs, Colo.), May 1980.

3. Siemers, Paul M. III: Shuttle Entry Technology Payloads. AAS Paper 75-251, Am. Astronaut. Soc., Aug. 1975.

4. Larson, Terry J.; and Schweikhard, William G.: Use of the Shuttle Entry Air Data Pressure System at Subsonic Speeds. Proc. 1978 Air Data Systems Conf. (Colorado Springs, Colo.), May 1978.

5. Siemers, Paul M. III; and Larson, Terry J.: Space Shuttle Orbiter and Aerodynamic Testing: J. Spacecraft and Rockets, vol. 16, no. 4, July-Aug. 1979, pp. 223-231.

6. Larson, Terry J.; and Siemers, Paul M. III: Use of Nose Cap and Fuselage Pressure Orifices for Determination of Air Data for Space Shuttle Orbiter Below Supersonic Speeds. NASA TP-1643, 1980.

7. Wolf, Henry; and Eades, J. B., Jr.: Analytical Techniques for the Reduction of Measurements From the Shuttle Entry Air Data System. Proc. 1978 Air Data Systems Conf. (Colorado Springs, Colo.), May 1978.

8. Wolf, Henry; Pruett, Dave; and Siemers, Paul M. III: Advances in Techniques for Flight Parameter Estimation From Shuttle Entry Air Data System (SEADS). Proc. 1980 Air Data Systems Conf. (Colorado Springs, Colo.), May 1980.

9. Schaefer, William T., Jr.: Characteristics of Major Active Wind Tunnels at the Langley Research Center. NASA TM X-1130, 1965.

10. Krisam, F.: Speed and Pressure Recording in Three-Dimensional Flow. NACA TM 688, 1932.

11. Bryer, D. W.; and Pankhurst, R. C.: Pressure-probe methods for determining wind speed and flow direction. Nat. Physical Lab., Her Majesty's Stationery Office (London), c.1971.

12. Montoya, Earl J.: Wind-Tunnel Calibration and Requirements for In-Flight Use of Fixed Hemispherical Head Angle-of-Attack and Angle-of-Sideslip Sensors. NASA TN D-6986, 1973.

13. Eshelby, M. E.: Flight Trials for the Calibration of Aircraft Primary Air Data Systems. Proc. 1978 Air Data Systems Conf. (Colorado Springs, Colo.), May 1978.

14. Larson, Terry J.; and Ehernberger, L. J.: Techniques Used for Determination of Static Source Position Error of a High Altitude Supersonic Airplane. NASA TM X-3152, 1975.

15. Yancey, Marion H., Jr.; and Martin, Reece S.: KC-135A Performance Test. AFFTC-TR-58-26, Air Force Flight Test Center, Edwards AFB, July 1958.

TABLE 1.—FLIGHT TEST MANEUVERS AND CONDITIONS

Maneuver	Primary test objective	Test condition	
		h_p, km	M
Constant Mach number, and pressure altitude	Static pressure calibration	3.0 7.6	0.29 to 0.86 ↓
Level acceleration and deceleration	Static pressure calibration and FADS variation with Mach number	3.0 4.6 7.6	0.39 to 0.86 ↓
Pullup (1.3g, 1.7g, 2.0g)	FADS variation with high angle of attack	3.0 4.6 7.6	0.40, 0.50, 0.60 0.40, 0.50, 0.60 0.50, 0.70, 0.78
Pushover (0g, 0.05g)	FADS variation with low angle of attack	3.0 4.6 7.6	0.40, 0.50, 0.60 0.40, 0.50, 0.60 0.50, 0.70, 0.78
Left and right sideslips	FADS variation with angle of sideslip	3.0 7.6	0.40, 0.50, 0.60 0.50, 0.70, 0.78

TABLE 2.—FLIGHT TEST INSTRUMENTATION MEASUREMENTS

Quantity	Range	Resolution	Estimated accuracy (2σ)
FADS pressures (orifices 1 to 18), kPa	±33.8	0.066	±0.3
Reference measurements—			
Airspeed, knots	0 to 750	0.7	±1.0
Altitude, m	0 to 18,300	3	±6
Angle of attack, deg	-6.2 to 27.1	0.03	±0.05
Angle of sideslip, deg	±15.0	0.03	±0.05
Longitudinal acceleration at center of gravity, g	-0.285 to 0.286	0.0006	±0.002
Lateral acceleration at center of gravity, g	-1.15 to 1.16	0.002	±0.008
Normal acceleration at center of gravity, g	-3 to 6	0.009	±0.021

TABLE 3.—FADS PRESSURE RATIO 2σ UNCERTAINTIES

Flight condition		FADS pressure measurement			
		p_i/p_t	$p_7/p_{21,22}$	p_6/p_1	$\Delta p_\alpha/q$, $\Delta p_\beta/q$
M	h_p, km	2σ uncertainty			
0.40	3.0	0.004 to 0.007	0.004	0.006	0.052
	4.6	0.005 to 0.008	0.005	0.007	0.075
0.50	3.0	0.004 to 0.007	0.004	0.006	0.048
	4.6	0.005 to 0.008	0.005	0.007	0.050
	7.6	0.007 to 0.012	0.007	0.010	0.067
0.60	3.0	0.004 to 0.006	0.005	0.005	0.035
	4.6	0.005 to 0.008	0.005	0.007	0.039
	7.6	0.007 to 0.011	0.007	0.010	0.050
0.70	7.6	0.006 to 0.011	0.006	0.009	0.040
0.78	7.6	0.008 to 0.010	0.006	0.009	0.025
0.85	7.6	0.006 to 0.010	0.006	0.008	0.021

TABLE 4. - RANGES OF DIFFERENCE BETWEEN FADS AND REFERENCE AIR DATA QUANTITIES FOR TWO TEST MANEUVERS

	Maneuver			
	Level acceleration		Pushover pullup	
	FADS configuration			
	Nose and fuselage orifices	Nose orifices only	Nose and fuselage orifices	Nose orifices only
	Differences between FADS and reference quantities			
ΔM, based on–				
Flight calibration	-0.001 to 0.010	-0.010 to 0.010	0.001 to 0.005	-0.008 to 0.010
Wind-tunnel calibration	-0.025 to -0.002	-0.026 to -0.006	-0.018 to -0.002	-0.010 to -0.001
Δh_p, m, based on–				
Flight calibration	0 to 55	-50 to 60	10 to 55	-15 to 55
Wind-tunnel calibration	-165 to -15	-170 to -35	-100 to -35	-80 to -30
$\Delta\alpha$, deg, using p_6, p_{12}, based on–				
Flight calibration	0.2 to 0.5	-0.1 to 0.4	-0.2 to 0.6	-0.7 to 0.5
Wind-tunnel calibration	-0.5 to 0.7	-0.5 to 0.6	-1.0 to 0	0.8 to -0.2
$\Delta\alpha$, deg, using p_3, p_{12}, based on–				
Flight calibration	-0.1 to 0.2	----------	-0.2 to 0.1	----------
Wind-tunnel calibration	----------	----------	----------	----------

TABLE 5. - ORIFICES RECOMMENDED FOR AIR DATA MEASUREMENTS

Air data quantity	FADS configuration			
	Nose and fuselage orifices		Nose orifices only	
	Orifices recommended on the basis of–			
	Flight tests	Wind-tunnel tests	Flight tests	Wind-tunnel tests
Total pressure	8	8	8	8
Mach number	7, (21, 22)	7, (21, 22)	1, 6	1, 6
Angle of attack	3, 12	6, 12	3, 12	6, 12
Angle of sideslip	14, 17*	13, 18	14, 17*	13, 18

*Flight data for orifices 13, 18 invalid.

ECN 11928

Figure 1. KC-135A test airplane.

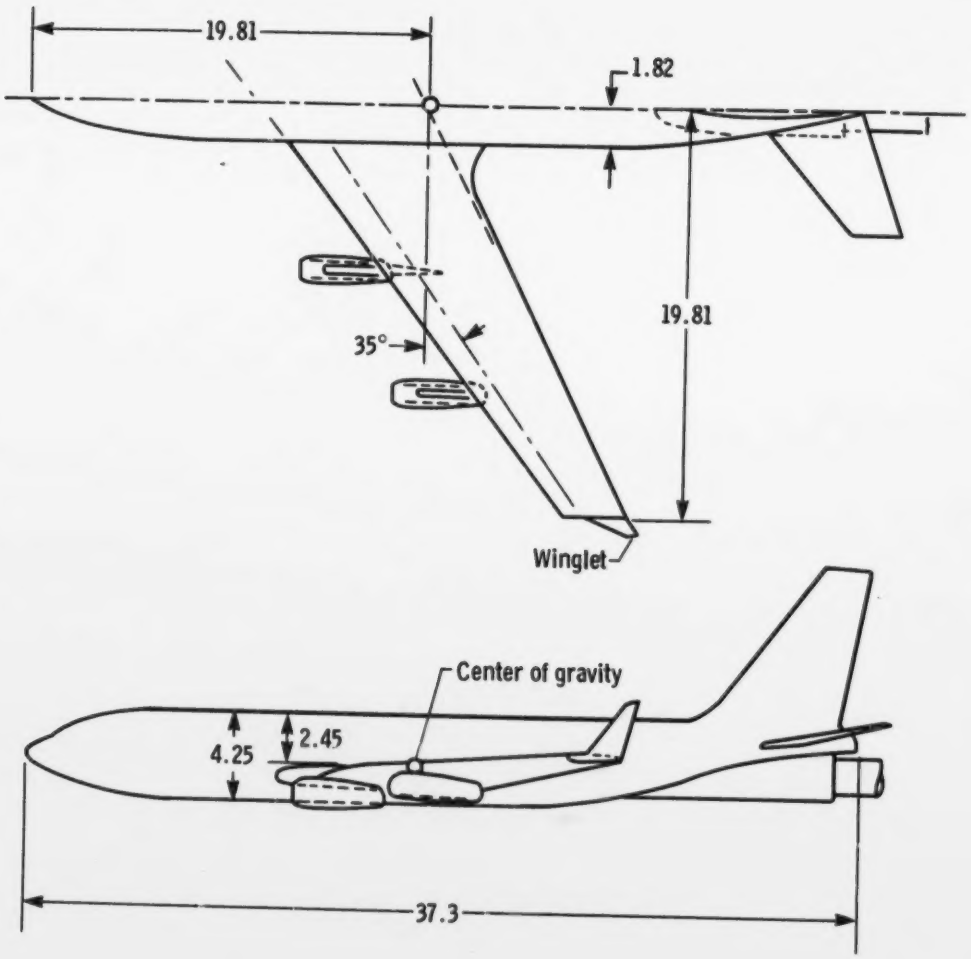

Figure 2. Dimensions of KC-135A airplane (in meters).

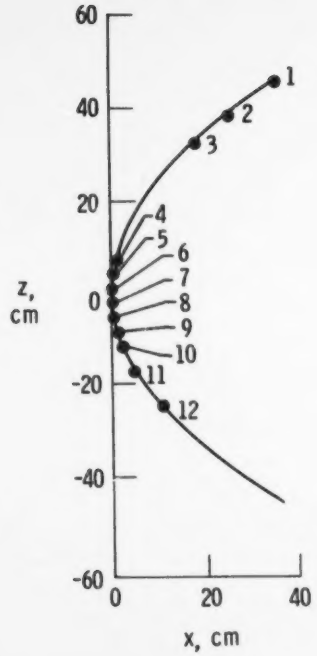

(a) FADS orifices in vertical plane.

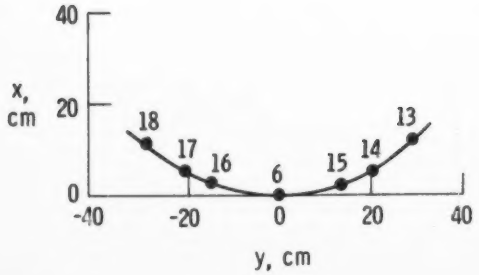

(b) FADS orifices in horizontal plane.

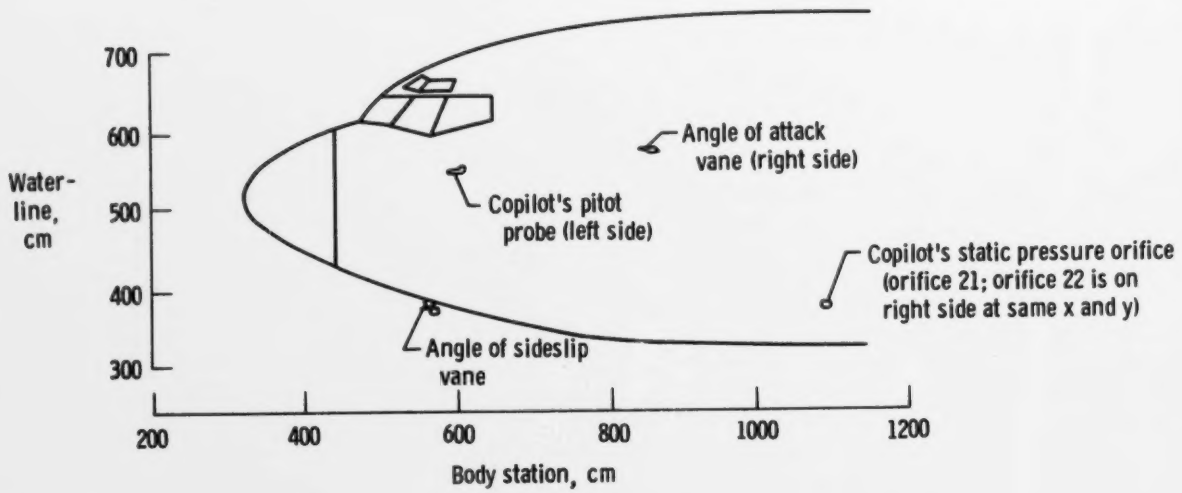

Figure 3. Location of FADS pressure orifices and reference air data sensors.

Figure 4. Winglet-equipped 0.035-scale model of KC-135A airplane.

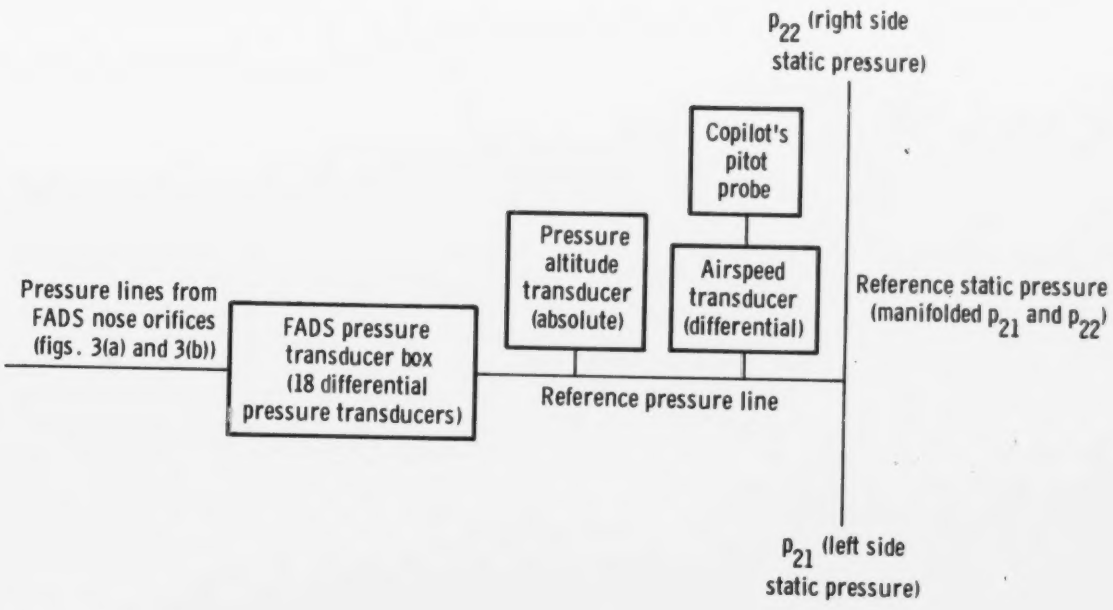
p_{22} (right side static pressure)
Copilot's pitot probe
Pressure altitude transducer (absolute)
Airspeed transducer (differential)
Pressure lines from FADS nose orifices (figs. 3(a) and 3(b))
FADS pressure transducer box (18 differential pressure transducers)
Reference pressure line
Reference static pressure (manifolded p_{21} and p_{22})
p_{21} (left side static pressure)

Figure 5. Aircraft pressure transducer measurements.

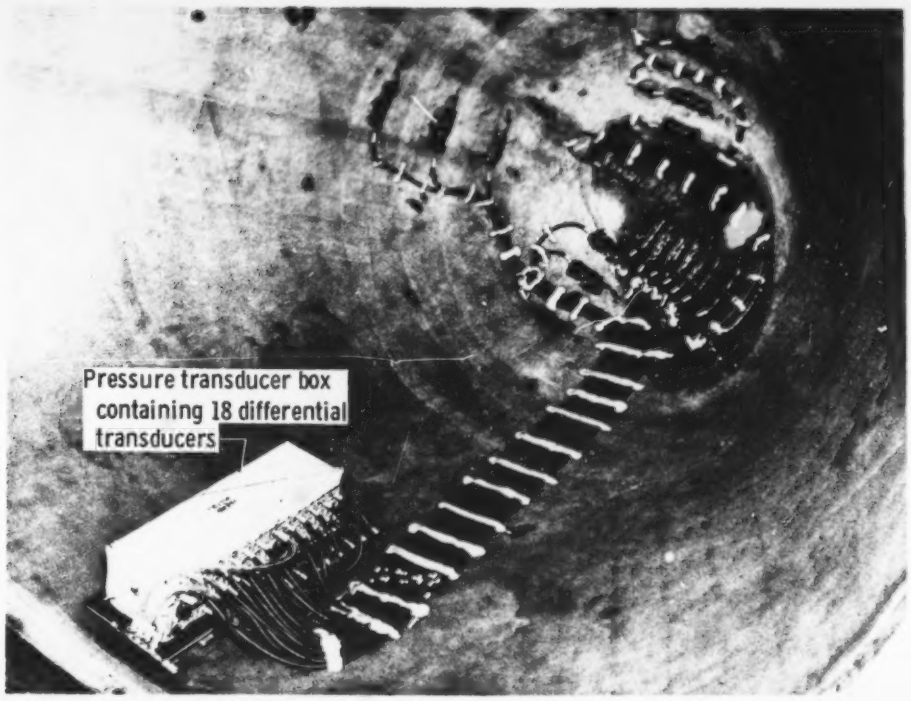

Figure 6. FADS pressure sensors and tubing in side nose section of airplane.

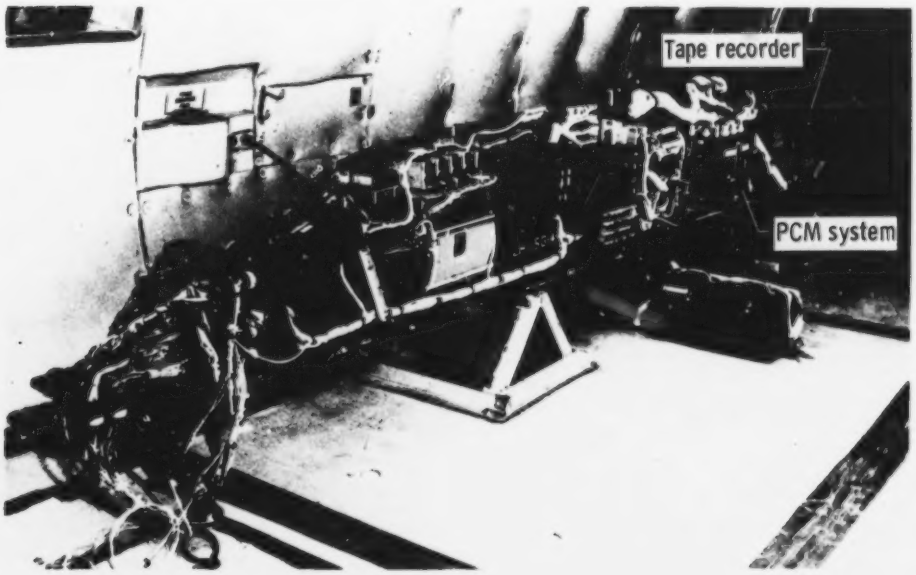

Figure 7. Data encoding and recording system.

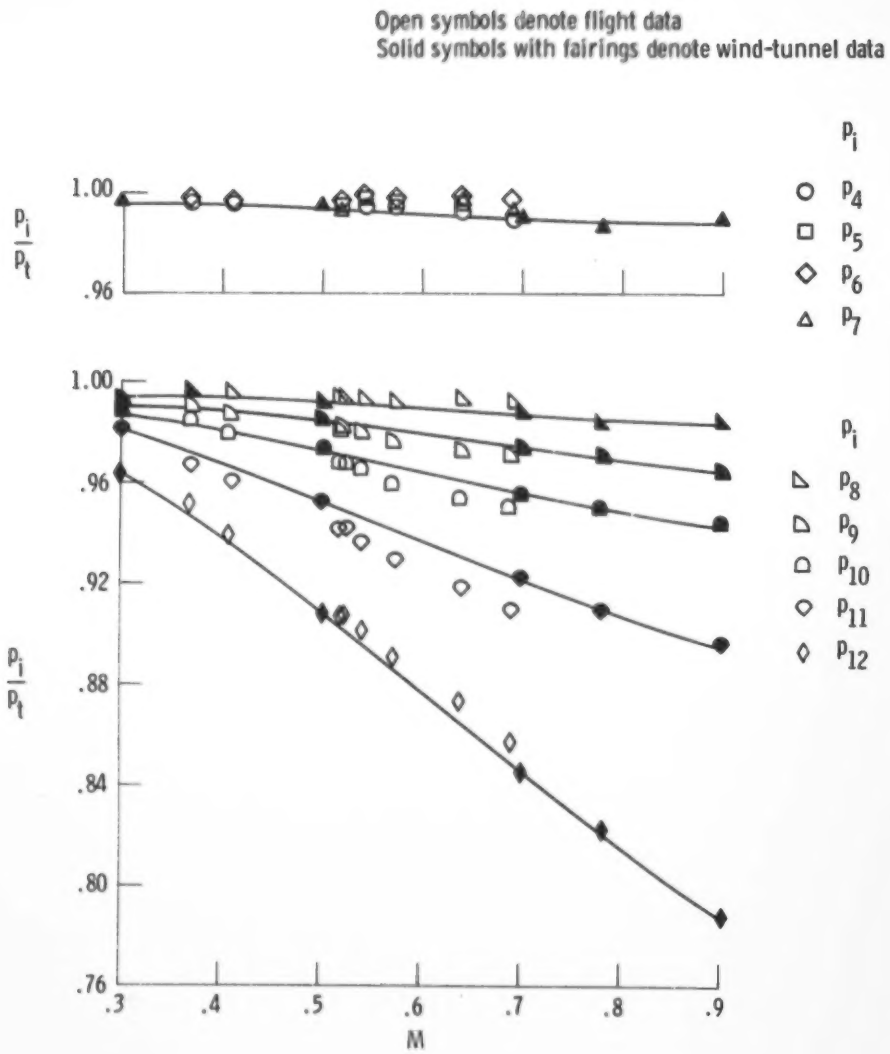

(a) $\alpha = -0.1°$.

Figure 8. Ratio of pressures measured in vertical plane of symmetry to total pressure. $\beta = 0°$.

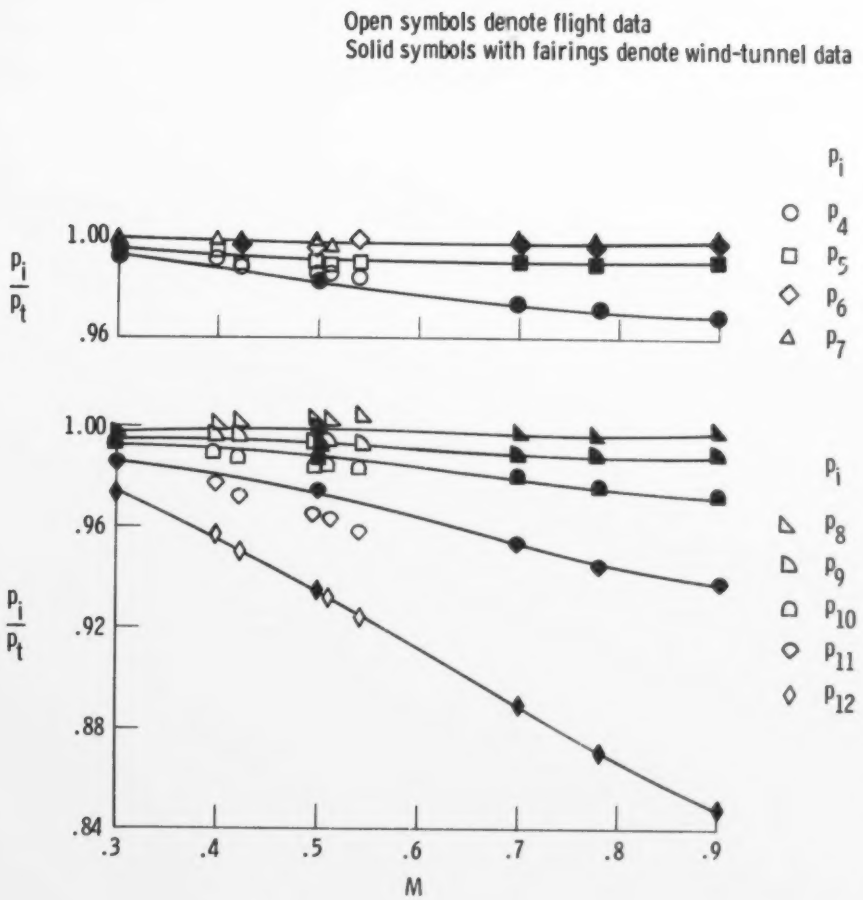

(b) $\alpha = 3.9°$.

Figure 8. Continued.

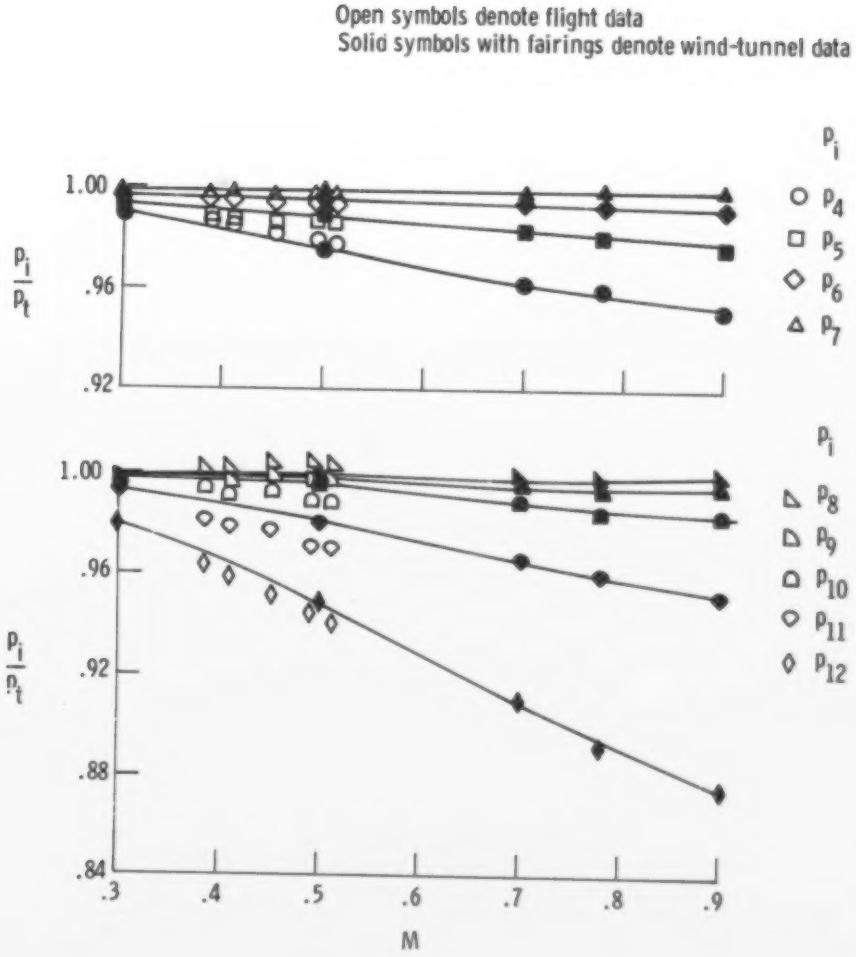

(c) $\alpha = 5.9°$.

Figure 8. Concluded.

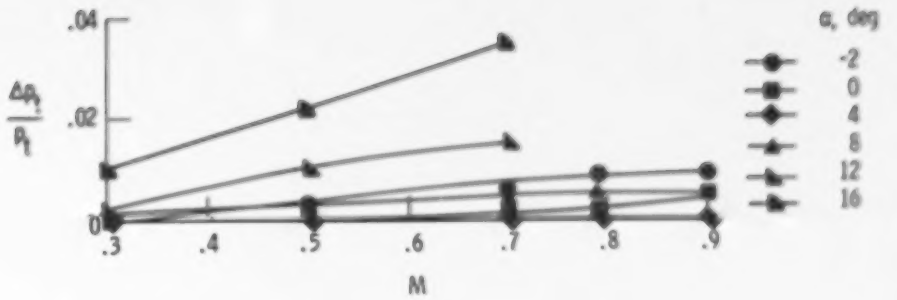

(a) $\Delta p_t = p_t - p_6$.

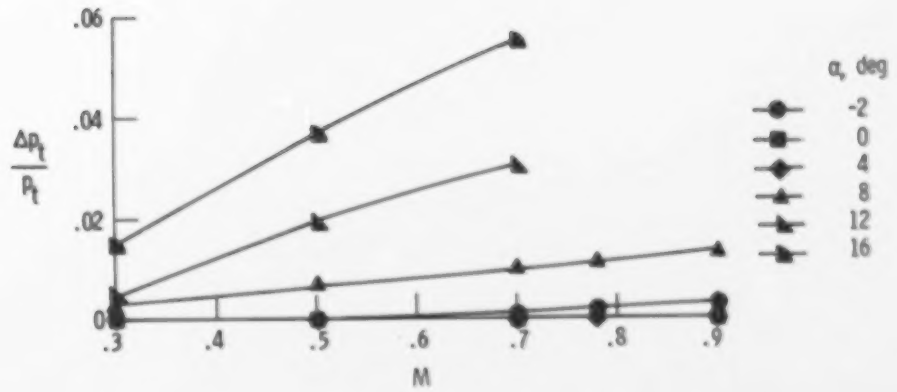

(b) $\Delta p_t = p_t - p_7$.

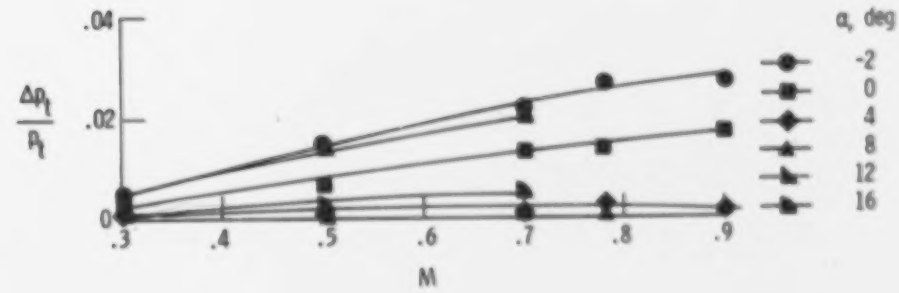

(c) $\Delta p_t = p_t - p_8$.

Figure 9. Total pressure correction for orifices 6, 7, and 8 at constant angles of attack as a function of Mach number. Wind-tunnel data; $\beta = 0°$.

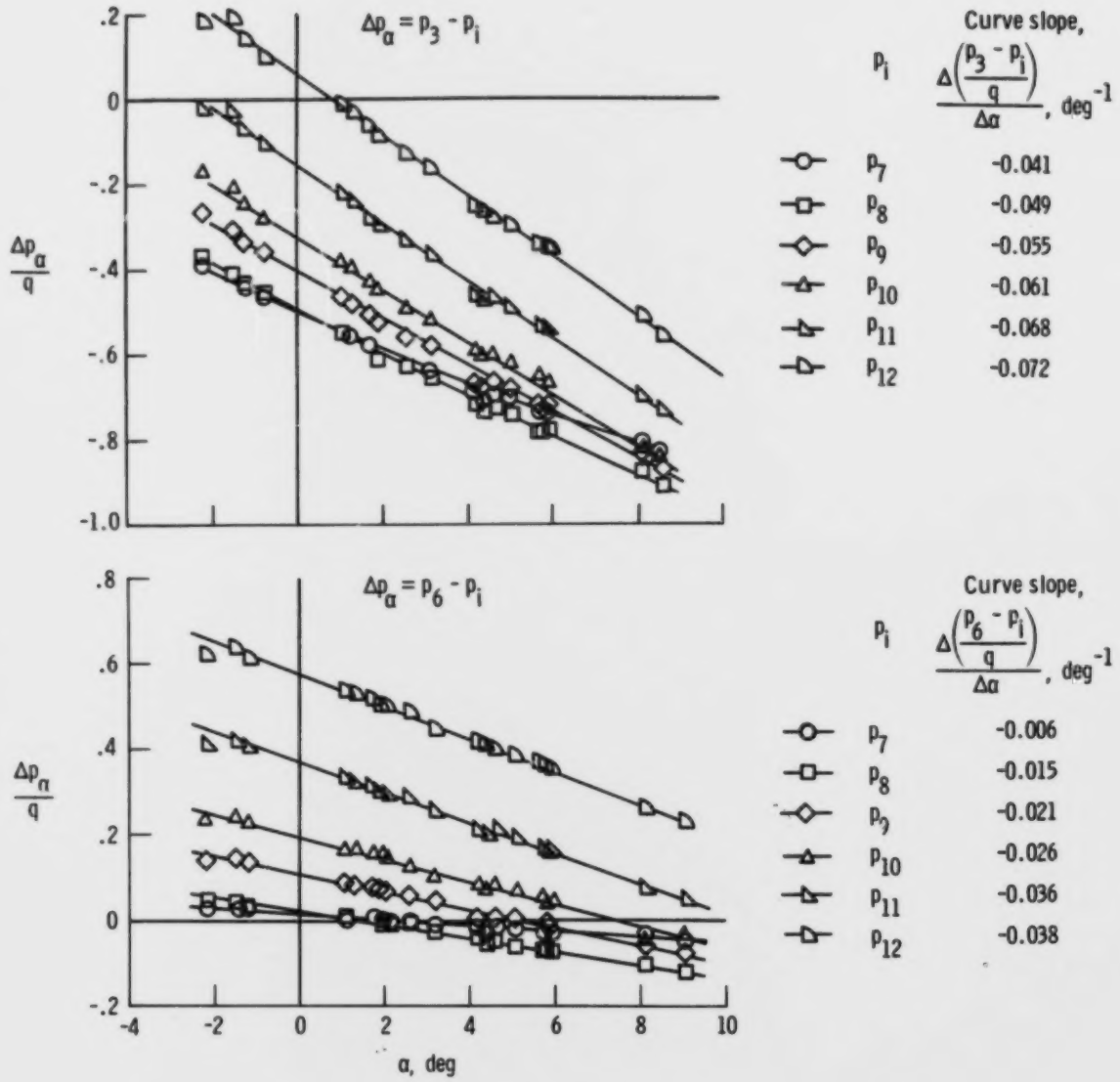

(a) M = 0.5.

Figure 10. Angle of attack pressure parameter for selected orifice pairs. Flight data; β = 0°.

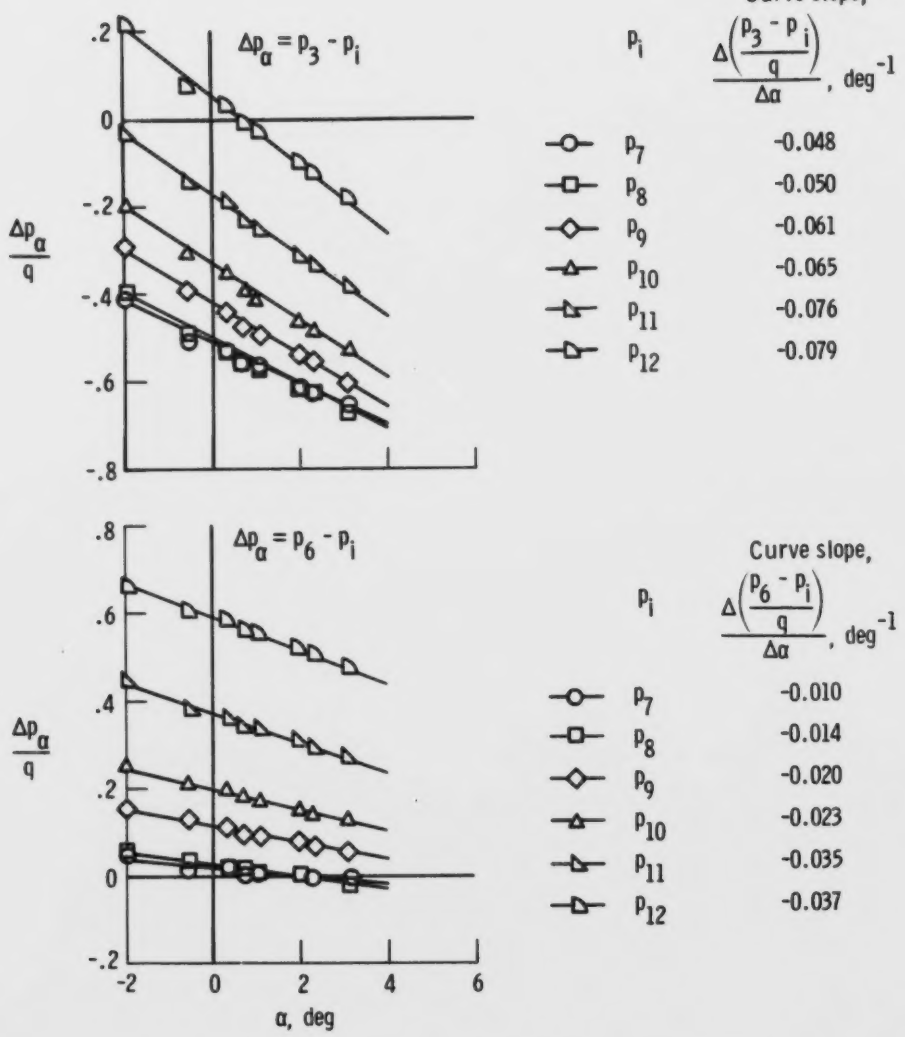

(b) M = 0.7.

Figure 10. Concluded.

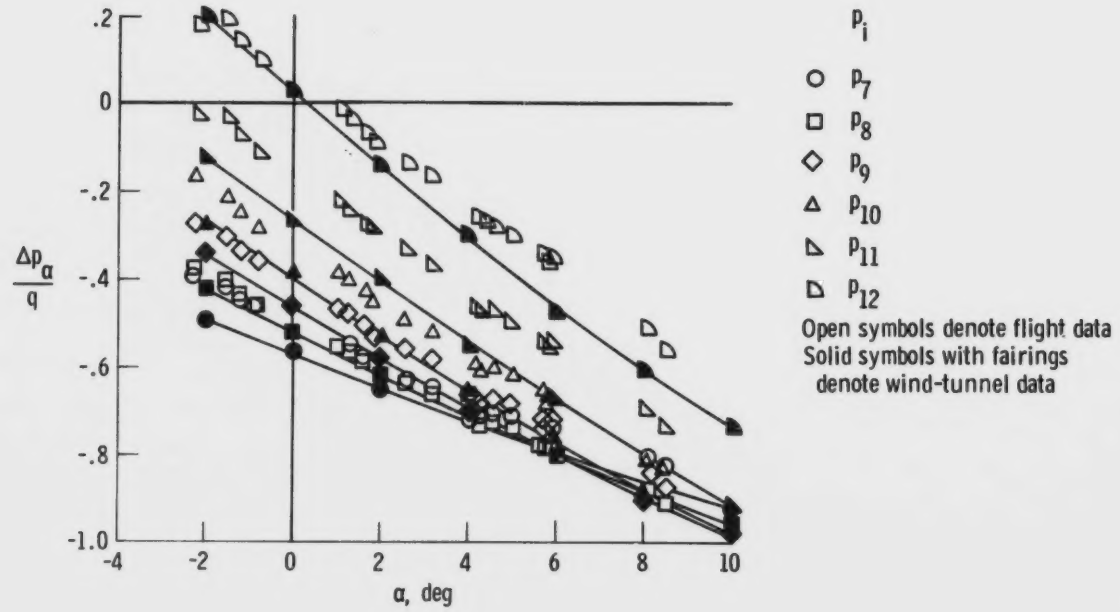

(a) $\Delta p_\alpha = p_3 - p_i$.

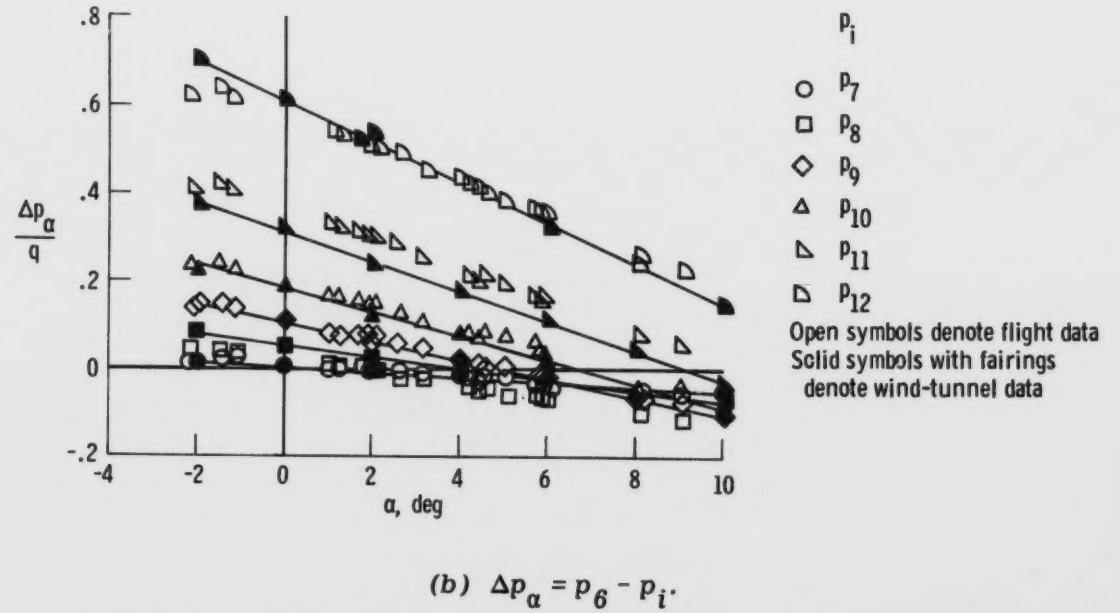

(b) $\Delta p_\alpha = p_6 - p_i$.

Figure 11. Angle of attack pressure parameter for selected orifice pairs. Flight and wind-tunnel data; $M = 0.5$; $\beta = 0°$.

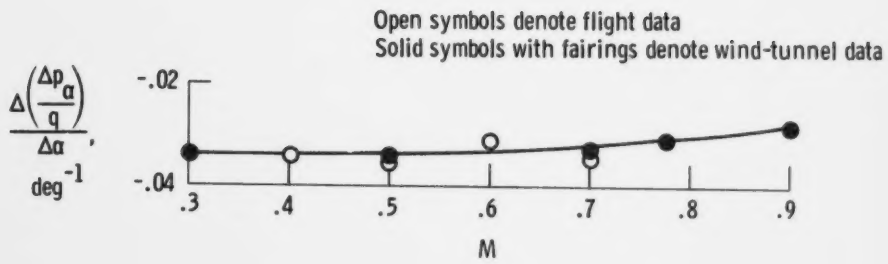

(a) $\Delta p_\alpha = p_6 - p_{11}$.

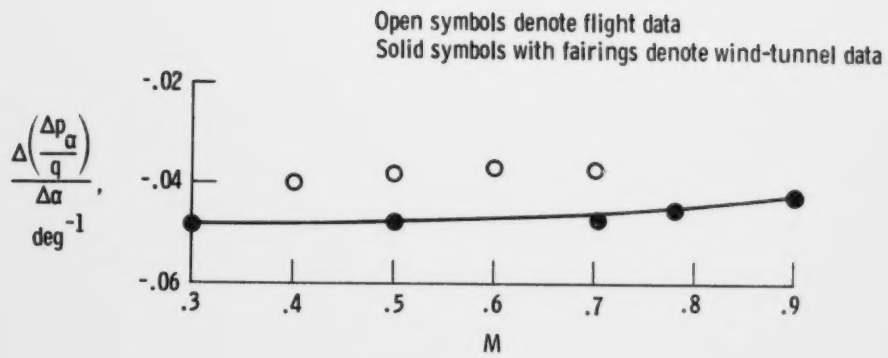

(b) $\Delta p_\alpha = p_6 - p_{12}$.

Figure 12. Sensitivity of angle of attack parameter to Mach number for pressure orifice pairs (6, 11) and (6, 12). $\beta = 0°$.

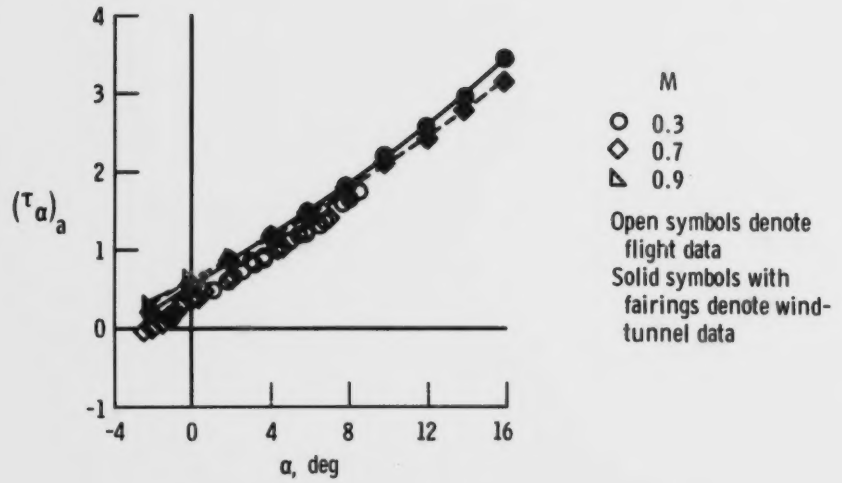

$$(a)\quad \tau_\alpha = \frac{p_{11} - p_3}{(p_6 - p_{11}) + 0.5(p_{11} - p_3)}.$$

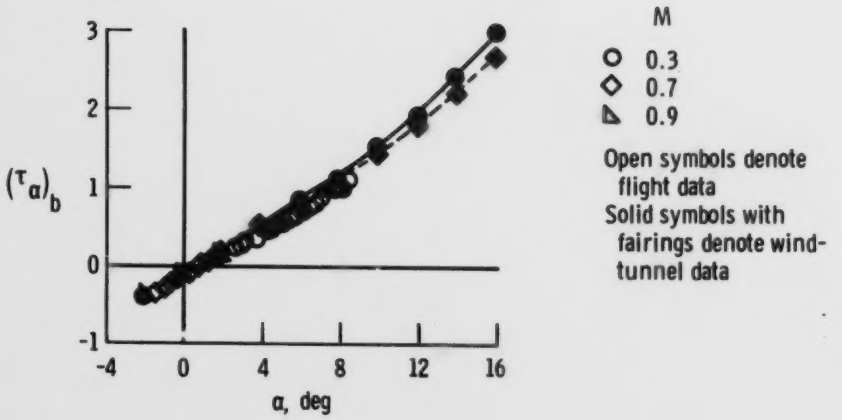

$$(b)\quad \tau_\alpha = \frac{p_{12} - p_3}{(p_6 - p_{12}) + 0.5(p_{12} - p_3)}.$$

Figure 13. τ_α pressure parameter plotted against angle of attack. $\beta = 0°$.

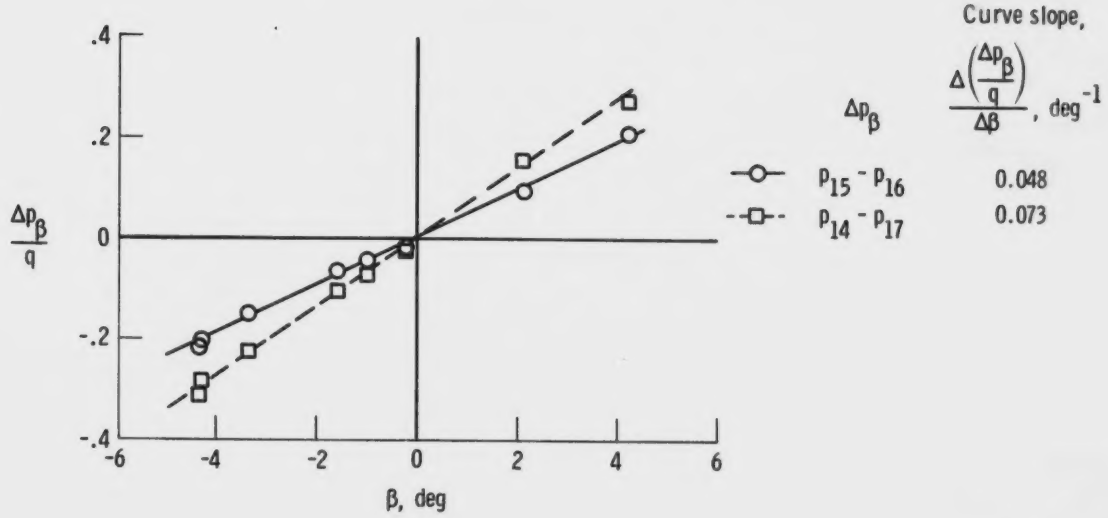

(a) M = 0.40.

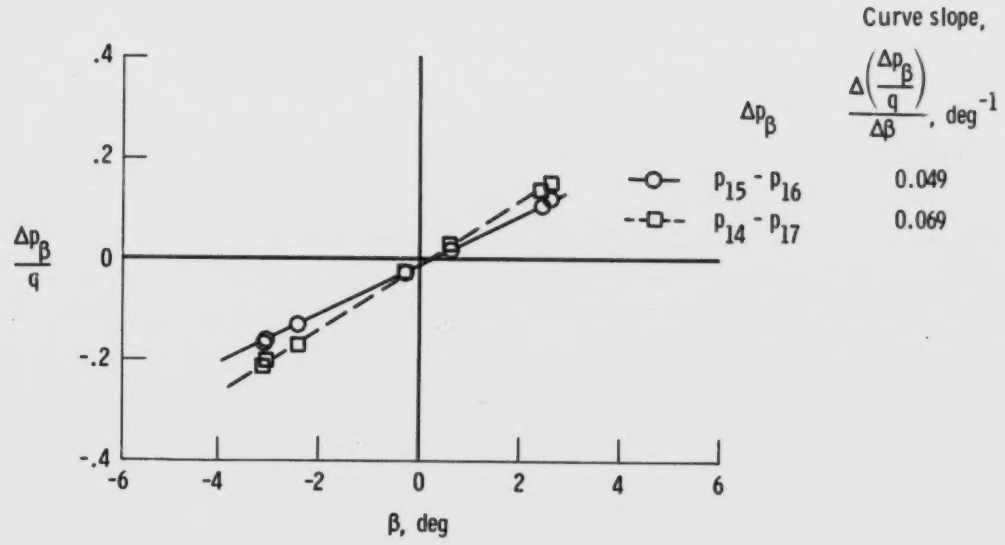

(b) M = 0.60.

Figure 14. Angle of sideslip pressure parameter for orifice pairs (15, 16) and (14, 17) plotted against angle of sideslip at selected Mach numbers. Flight data.

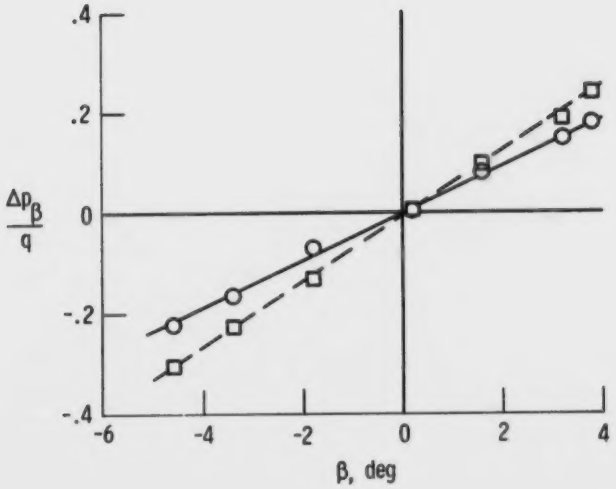

Δp_β	Curve slope, $\frac{\Delta\left(\frac{\Delta p_\beta}{q}\right)}{\Delta\beta}$, deg^{-1}
$p_{15} - p_{16}$	0.047 (0.048)
$p_{14} - p_{17}$	0.065 (0.069)

(Parentheses indicate wind-tunnel values)

(c) M = 0.70.

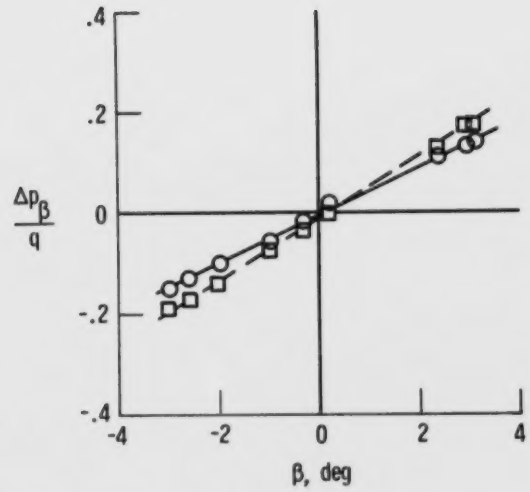

Δp_β	Curve slope, $\frac{\Delta\left(\frac{\Delta p_\beta}{q}\right)}{\Delta\beta}$, deg^{-1}
$p_{15} - p_{16}$	0.047 (0.043)
$p_{14} - p_{17}$	0.065 (0.068)

(Parentheses indicate wind-tunnel values)

(d) M = 0.78.

Figure 14. Concluded.

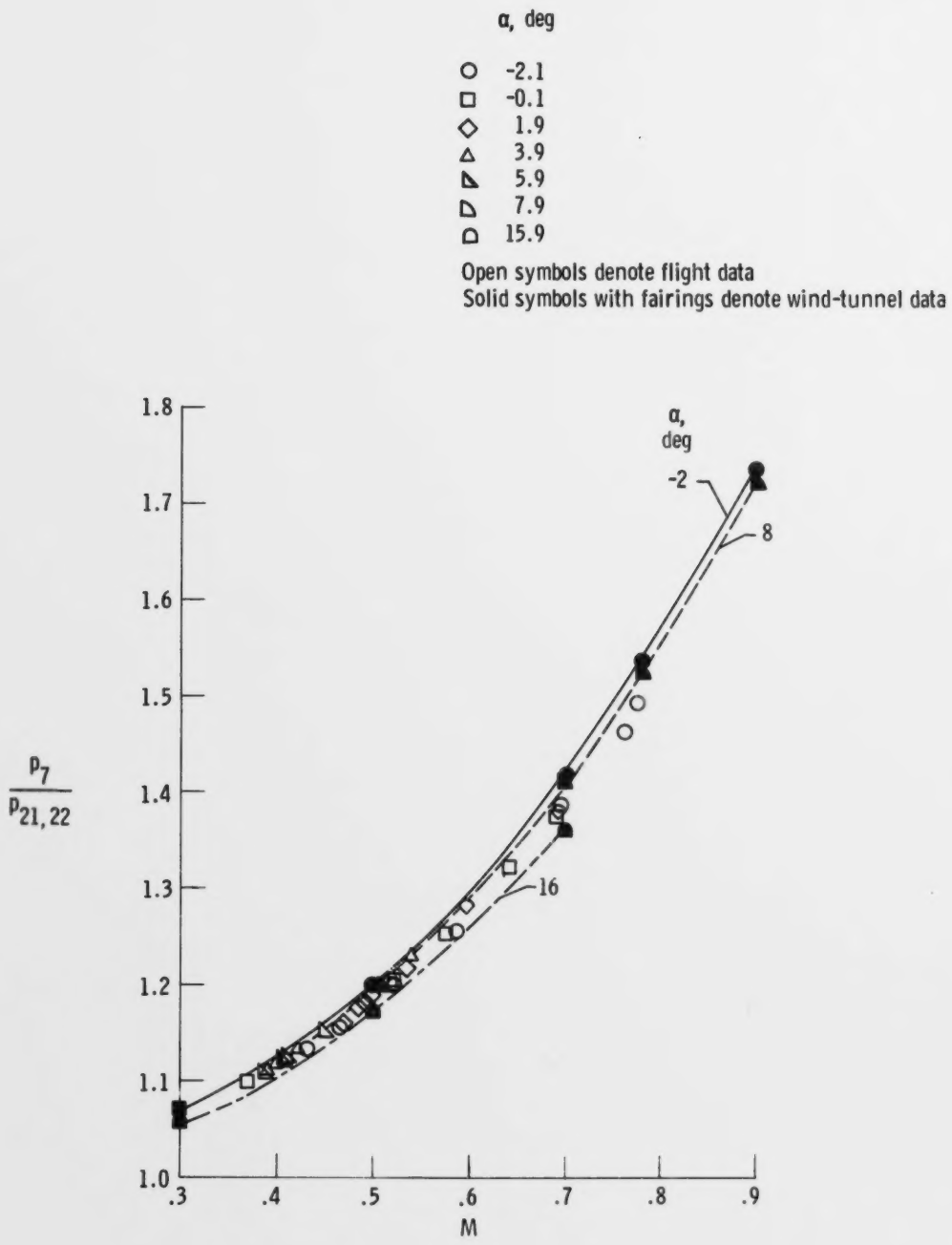

Figure 15. Pressure ratio for determination of Mach number for a combination of nose and fuselage pressure orifices. β = 0°.

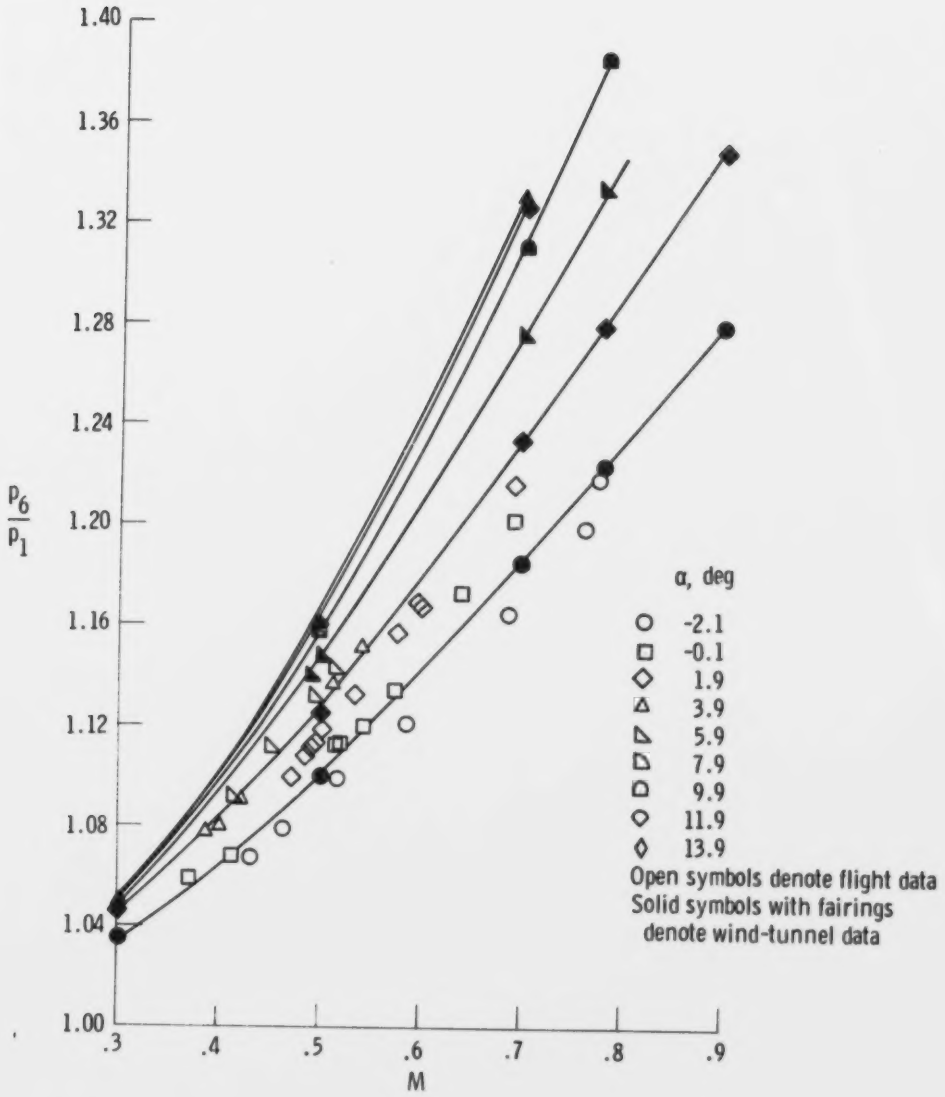

Figure 16. Pressure ratio for determination of Mach number using orifices on nose only. β = 0°.

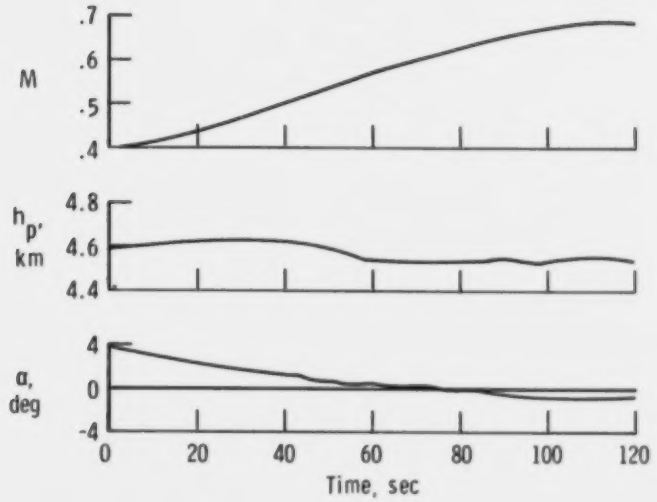

(a) Level acceleration maneuver.

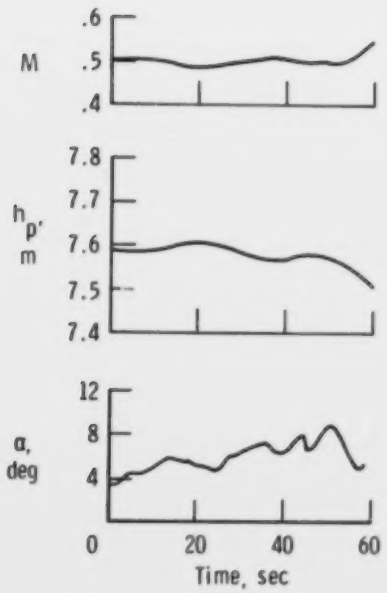

(b) Pushover pullup maneuver.

Figure 17. Quantities obtained from reference flight air data system during level acceleration and pushover pullup maneuvers.

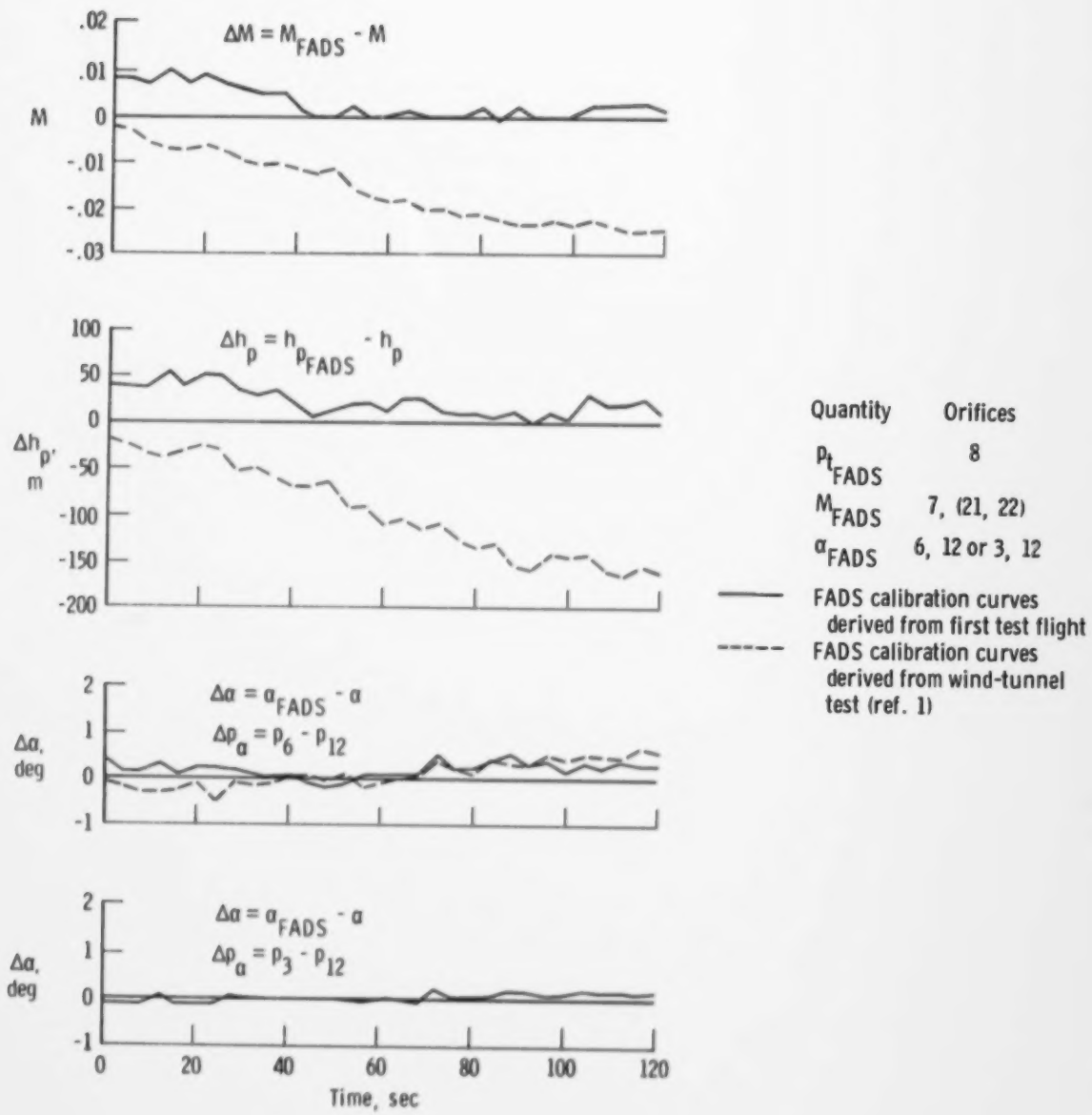

(a) Comparison with FADS using both nose and fuselage orifices.

Figure 18. Comparison between air data quantities derived from FADS and reference system during level acceleration maneuver.

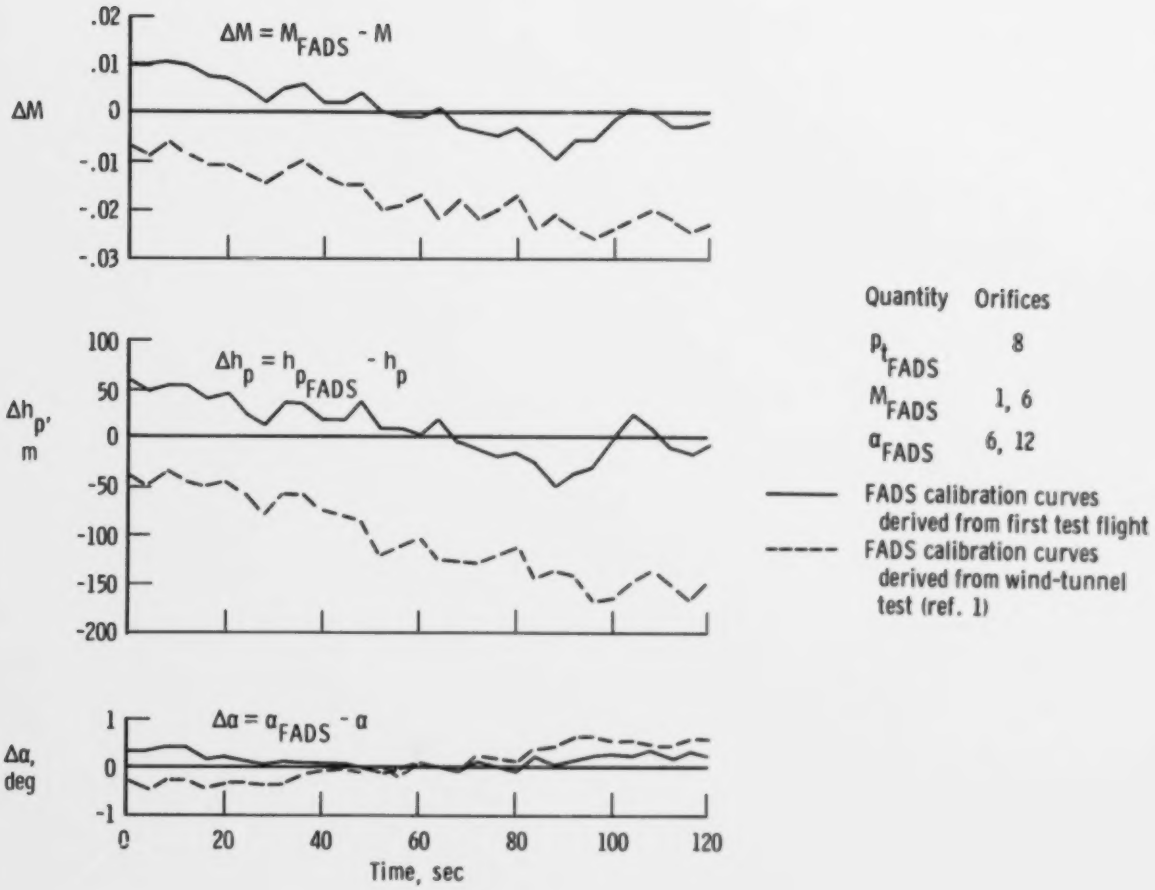

(b) Comparison with FADS using nose orifices only.

Figure 18. Concluded.

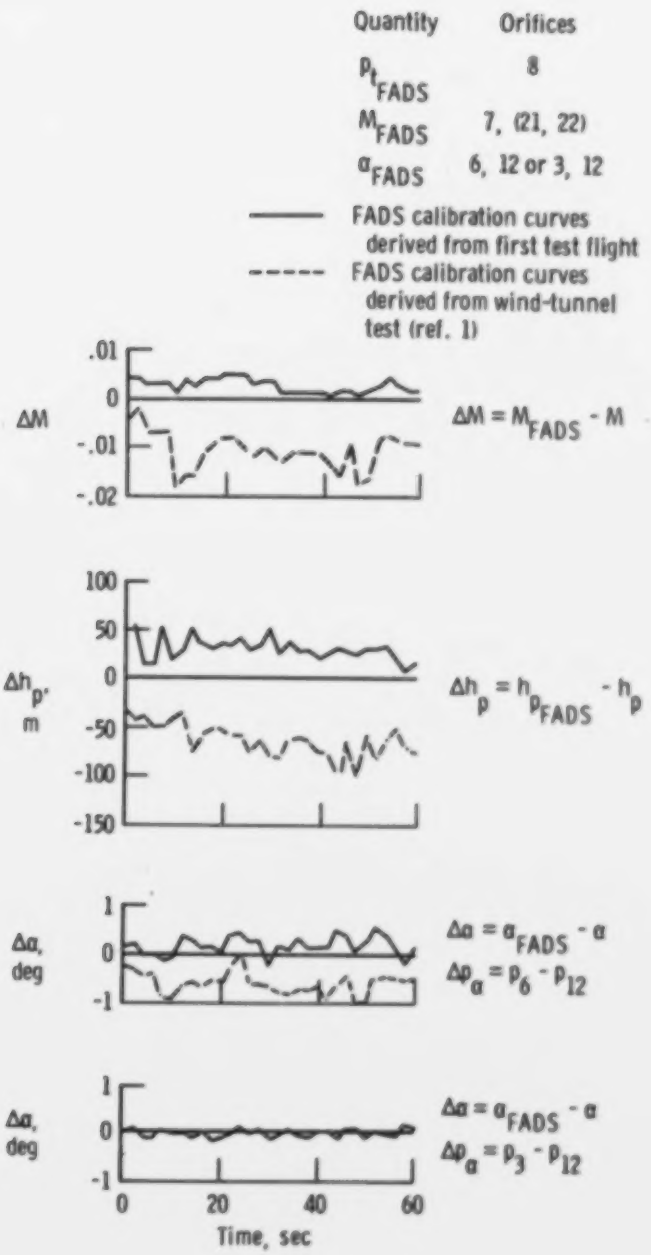

(a) Comparison with FADS using both nose and fuselage orifices.

Figure 19. Comparison between air data quantities derived from FADS and reference system during pushover pullup maneuver.

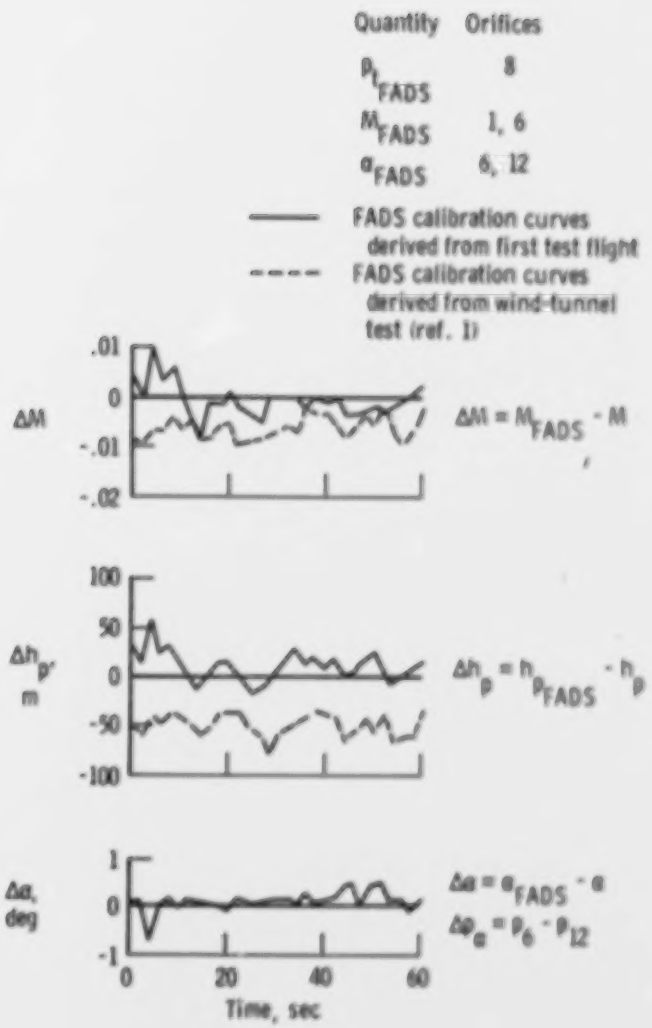

(b) Comparison with FADS using nose orifices only.

Figure 19. Concluded.

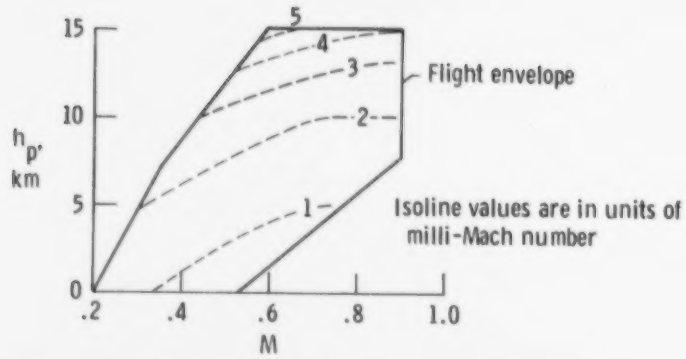

(a) Mach number errors.

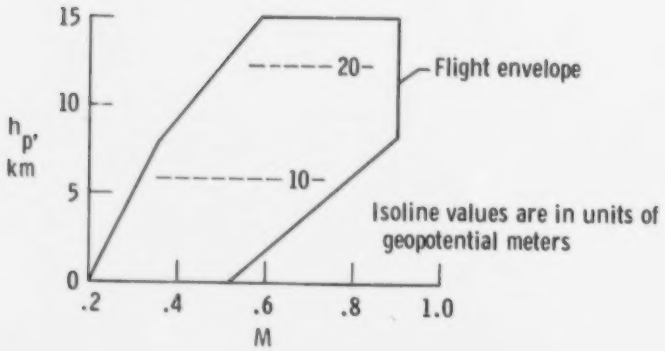

(b) Pressure altitude errors.

Figure 20. Mach number and pressure altitude errors for an "optimum" pitot-static system used within the Mach number/pressure altitude flight envelope of the KC-135A airplane.

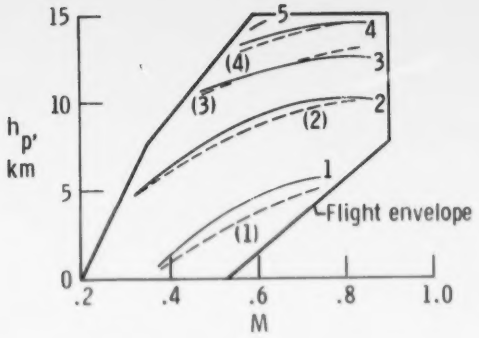

Isoline values are in units of milli-Mach number

Quantity	Orifice
p_t	8
M	7, (21, 22)
α	6, 12

Solid lines denote FADS
Dashed lines denote "optimum" system

(a) Mach number errors.

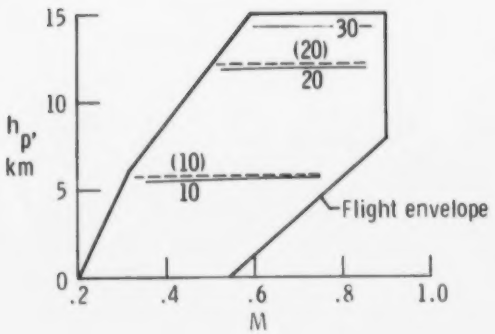

Isoline values are in units of geopotential meters

Quantity	Orifice
p_t	8
M	7, (21, 22)
α	6, 12

Solid lines denote FADS
Dashed lines denote "optimum" system

(b) Pressure altitude errors.

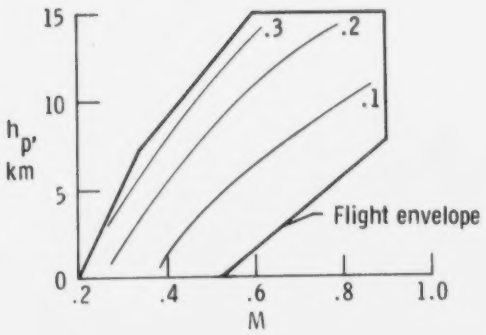

Isoline values are in units of degrees

Quantity	Orifice
p_t	8
M	7, (21, 22)
α	6, 12

(c) Angle of attack errors.

Figure 21. Mach number, pressure altitude, and angle of attack errors for a FADS configuration that uses both nose and fuselage orifices. $\alpha = 8°$.

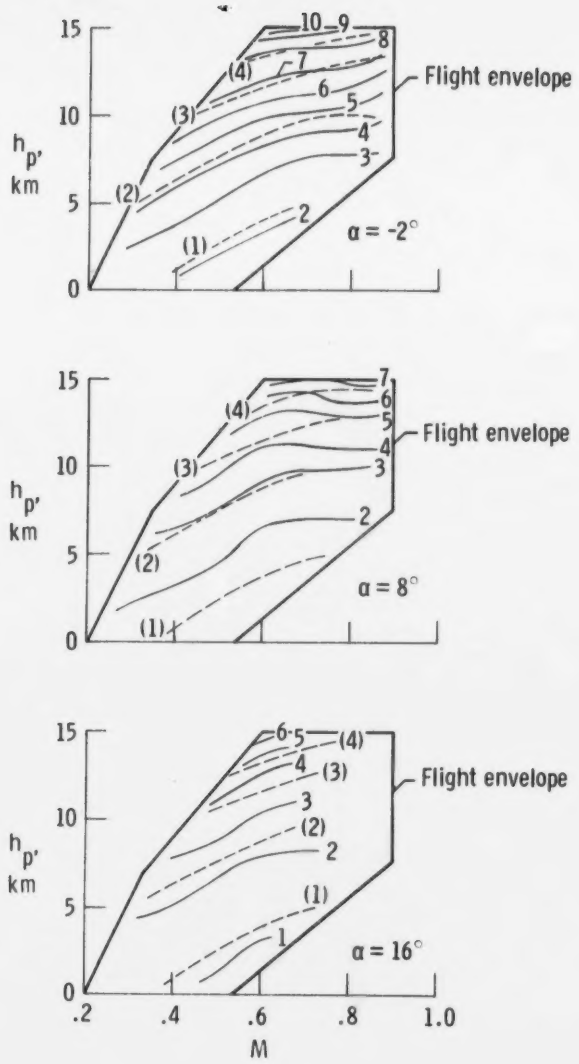

Quantity	Orifice
p_t	8
M	1, 6
α	6, 12

Solid lines denote FADS
Dashed lines denote "optimum" system

Isoline values are in units of milli-Mach number

(a) Mach number errors.

Figure 22. Mach number, pressure altitude, and angle of attack errors for an all-nose-orifice FADS configuration.

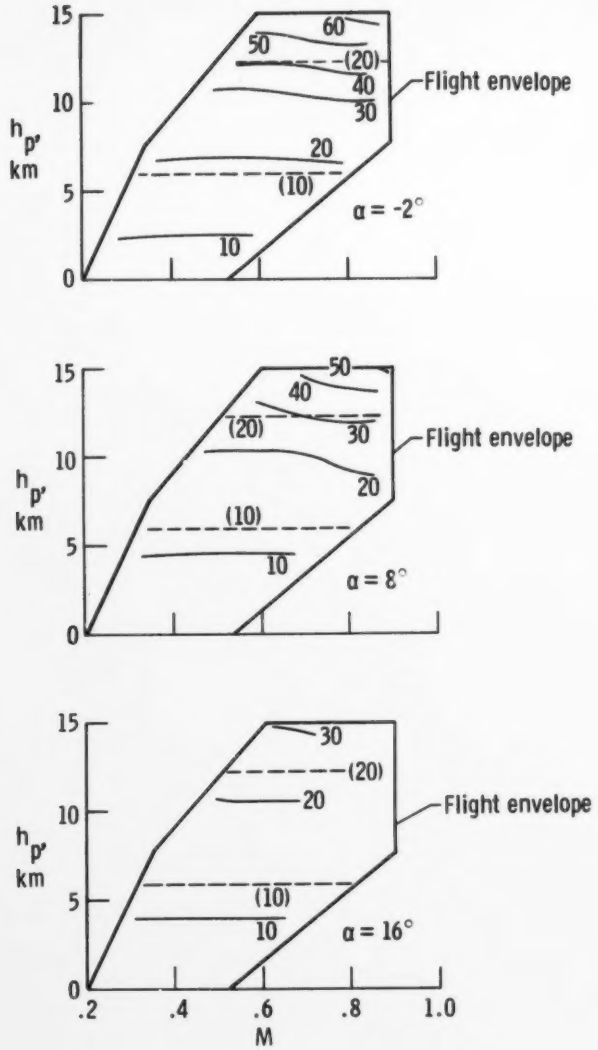

Quantity	Orifice
p_t	8
M	1, 6
α	6, 12

Solid lines denote FADS
Dashed lines denote "optimum" system

Isoline values are in units of milli-Mach number

(b) Pressure altitude errors.

Figure 22. Continued.

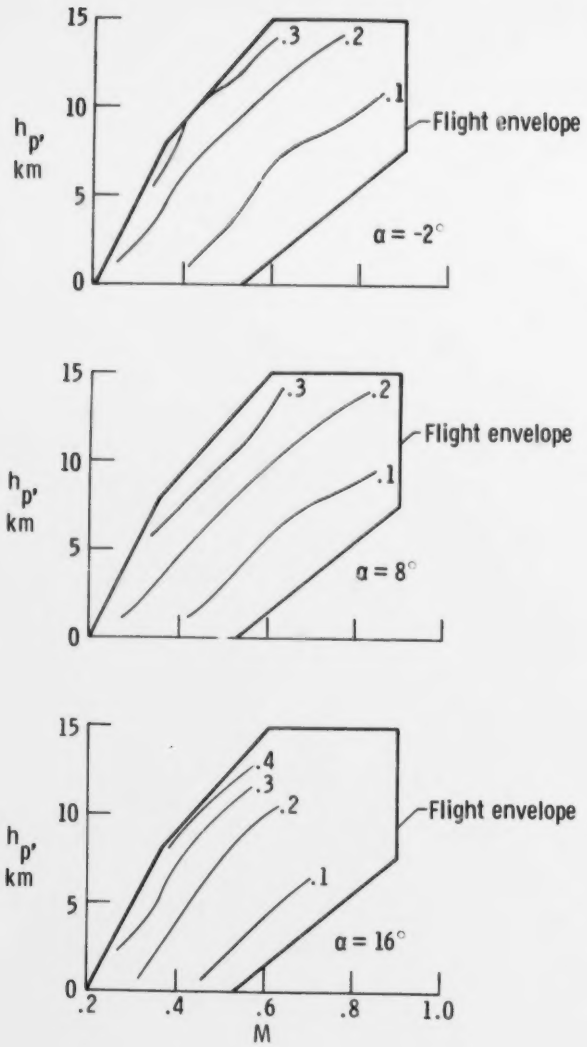

Quantity	Orifice
p_t	8
M	1, 6
α	6, 12

Isoline values are in units of milli-Mach number

(c) Angle of attack errors.

Figure 22. Concluded.

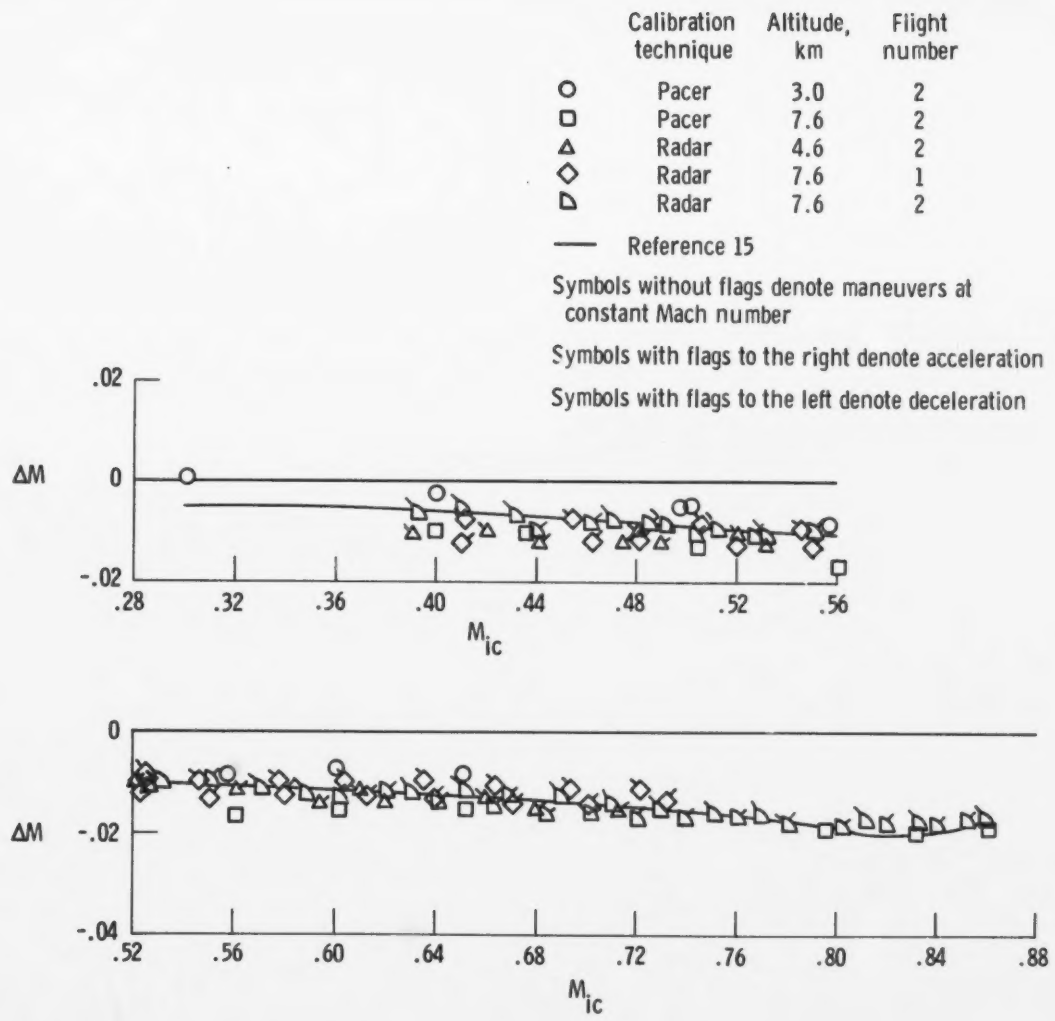

Figure 23. Mach number corrections for static pressure position error (orifices 21 and 22) for FADS flight tests. α = 0° to 9°; radar used is an FPS-16.

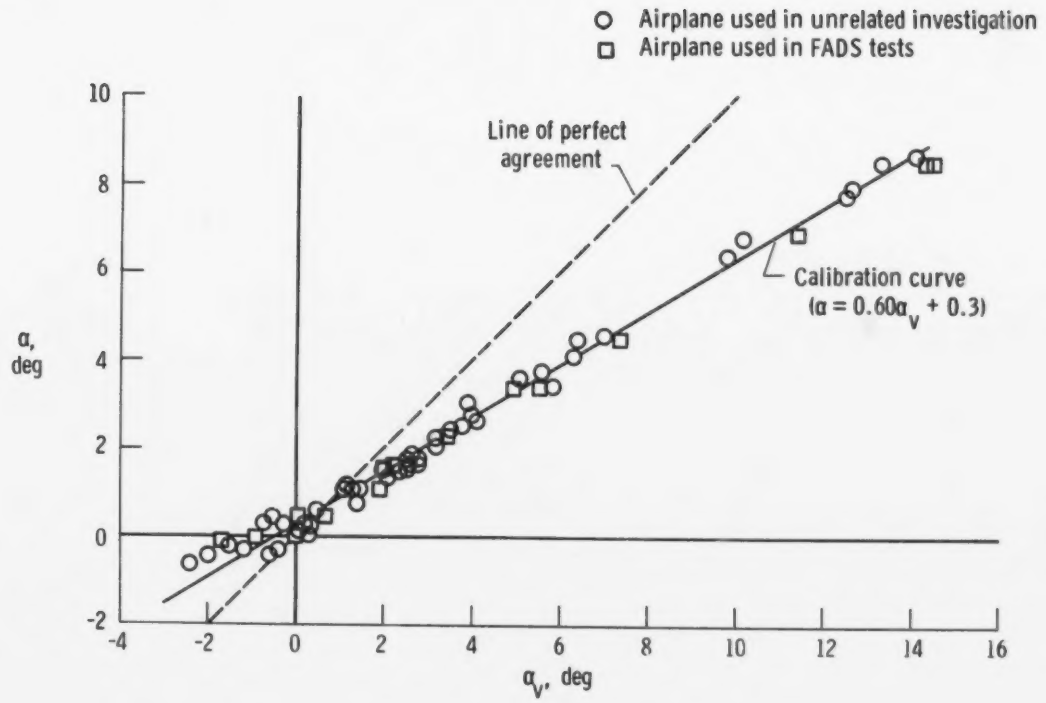

Figure 24. Angle of attack calibration for reference vane.

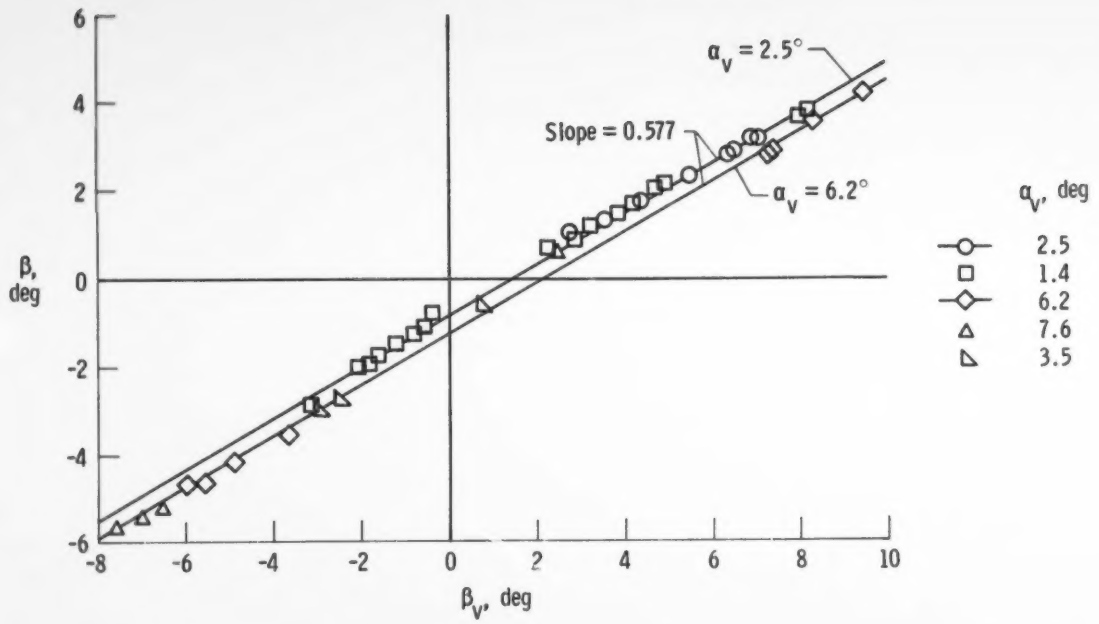

Figure 25. Angle of sideslip calibration for reference vane at constant α_V. Data are from airplane used in separate tests. M = 0.24 to 0.45.

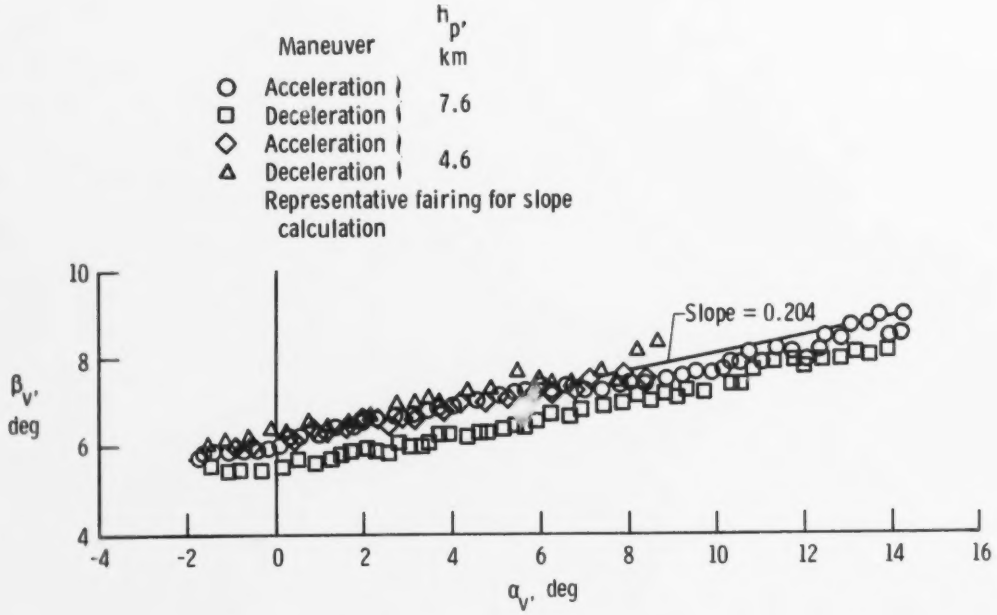

Figure 26. Variation of angle of sideslip correction for reference vane with vane angle of attack. Data are from airplane used in FADS tests.

1. Report No. NASA TP-1871	2. Government Accession No.	3. Recipient's Catalog No.
4. Title and Subtitle SUBSONIC TESTS OF AN ALL-FLUSH-PRESSURE-ORIFICE AIR DATA SYSTEM		5. Report Date June 1981 6. Performing Organization Code RTOP 506-51-34
7. Author(s) Terry J. Larson and Paul M. Siemers III		8. Performing Organization Report No. H-1122 10. Work Unit No.
9. Performing Organization Name and Address Dryden Flight Research Center P.O. Box 273 Edwards, California 93523		11. Contract or Grant No.
12. Sponsoring Agency Name and Address National Aeronautics and Space Administration Washington, D.C. 20546		13. Type of Report and Period Covered Technical Paper 14. Sponsoring Agency Code

15. Supplementary Notes

This paper is a revised and expanded version of "Subsonic Investigation of an All Flush Orifice Air Data System," a paper presented by the authors at the 1980 Air Data Systems Conference (Colorado Springs, Colo.) in May, 1980.

Terry J. Larson: Dryden Flight Research Center Paul M. Siemers III: Langley Research Center

16. Abstract

The use of an all-flush-pressure-orifice array as a subsonic air data system was evaluated in flight and wind-tunnel tests. Two orifice configurations were investigated. Both used orifices arranged in a cruciform pattern on the airplane nose. One configuration also used orifices on the sides of the fuselage for a source of static pressure. The all-nose-orifice configuration was similar to the shuttle entry air data system (SEADS). The flight data were obtained with a KC-135A airplane. The wind-tunnel data were acquired with a 0.035-scale model of the KC-135A airplane.

With proper calibration, several orifices on the vertical centerline of the vehicle's nose were found to be satisfactory for the determination of total pressure and angle of attack. Angle of sideslip could be accurately determined from pressure measurements made on the horizontal centerline of the aircraft. Orifice pairs were also found that provided pressure ratio relationships suitable for the determination of Mach number. The comparisons in the study indicated the accuracy that can be expected for the air data determined with SEADS during subsonic orbiter flight.

17. Key Words (Suggested by Author(s))	18. Distribution Statement
Flush pressure orifices Flush air data system Flow angularity measurements Air data Airspeed and altitude measurements	Unclassified—Unlimited Subject category 06

19. Security Classif. (of this report)	20. Security Classif. (of this page)	21. No. of Pages	22. Price*
Unclassified	Unclassified	50	A03

*For sale by the National Technical Information Service, Springfield, Virginia 22161

NASA-Langley, 1981